20% More Eelgrass by 2020
Task 2 Technical Memorandum

Final Draft

Kate Buenau
Lyle Hibler
Tarang Khangaonkar
Wen Long
Dana Woodruff
Ron Thom

Contents

Introduction

Our objectives for this task were to develop a model for eelgrass *Zostera marina* that could be applied across Puget Sound to determine which areas would be most suitable for restoring eelgrass. Finding suitable sites requires some form of model that integrates key environmental factors including temperature, light availability, tide ranges, and salinity. In some cases site selection has been based on limited information about habitat quality (e.g. Short et al. 2002) due to the lack of more extensive environmental data. In Puget Sound, however, we have a hydrodynamic and water quality model that models temperature, salinity, water depth and other environmental characteristics based on weather, freshwater and nutrient inputs, and other forcing factors. This model provides time series of water quality for thousands of locations throughout Puget Sound. While this information could be used to inform a static habitat suitability model, it also allows us to use a dynamic model of eelgrass biomass over the course of a year, more effectively integrating the range and variability of conditions at individual sites.

Several types of models have been developed to model the dynamics of seagrass biomass, but most have been for other species (Burd and Dunton 2001, Eldridge et al. 2004) or for *Z. marina* in other regions (Bocci et al. 1997, Zharova et al. 2001, Aveytua-Alcazar et al. 2008, Carr et al. 2012). The Eldridge and Kaldy (2004) model has been parameterized for *Z. marina* in Yaquina Bay, OR, (Kaldy and Eldridge 2006) but model development was not completed. We used the Eldridge and Kaldy (2004) model as a starting point and made further adaptations, including the incorporation of Puget Sound data when available and appropriate. While initially we planned on parameterizing the existing model with data from Puget Sound, we found that based upon the data available and output from early versions of the model that it would be beneficial to make some updates to functional forms in the model as well. Therefore, as presented here the model includes updates to metabolic functions (photosynthesis and respiration) and their dependence upon light, temperature, and salinity. We will apply this model along with additional site selection criteria (to be described elsewhere) to help select sites for further consideration for eelgrass planting suitability. While we have a working model that has improved throughout the course of its development for this project, this model has significant further potential for ongoing development to better model eelgrass dynamics, determine site suitability, and identify research priorities.

Methods

In this section we will first describe the Puget Sound hydrodynamic and water quality model, then explain how the output of this model is processed for use in the eelgrass biomass model. We then explain how the biomass model is structured and parameterized, how simulations are run, and how model output was compared to DNR monitoring data.

Puget Sound Hydrodynamic Model

PNNL has developed a predictive model for simulating hydrodynamics (tidal circulation; Yang and Khangaonkar 2010) and biogeochemical cycles (water quality; Khangaonkar et al. 2012) in the Puget

Sound and Georgia Basin. This model, referred to as the PSGB model, was used to generate physical oceanographic and biogeochemical information for the Year 2007 selected for this eelgrass study. The model results were saved at a six-hour time step in three-dimensional spatial resolution and were subsequently processed for use in the eelgrass model (see *Use of PSGB model…* below). The calibration of the model was based on 2006 data. Presented in the following sections is an application of the model for the year 2007 selected for use in this eelgrass assessment.

The PSGB model consists of two major components: 1) a three-dimensional coastal hydrodynamic model and 2) a water quality model. The model was constructed using the unstructured grid Finite Volume Coastal Ocean Model (FVCOM) framework (Chen et al. 2003) and the integrated compartment model (CE-QUAL-ICM) for biogeochemical water quality kinetics developed by U.S. Army Corps of Engineers (Cerco and Cole 1994). The eelgrass model currently uses water elevation, water temperature, and salinity, which are calculated using the FVCOM model. The CE-QUAL-ICM model includes nutrients, dissolved organic matter, dissolved oxygen, and two species of microalgae. While the eelgrass model does not currently employ these variables, they are available if useful in the future.

The hydrodynamic component of the PSGB model has been discussed in detail previously (Khangaonkar et al. 2011). Figure 1 shows the unstructured model grid constructed using triangular cells with higher resolution in narrower regions of the Salish Sea, growing coarser in the Strait of Juan de Fuca with up to 3-km resolution near the open boundaries. The grid resolution is, on average, 250 m in the inlets and bays and approximately 800 m inside the Puget Sound main basin and consists of 9,013 nodes and 13,941 elements. A sigma-stretched coordinate system was used in the vertical plane with 10 terrain-following sigma layers distributed with more layer density near the surface.

The ocean-side open boundary is located just west of the Strait of Juan de Fuca, while the second open boundary is located near the northernmost point of the Georgia Strait (Canadian waters) near Johnstone Strait. The model is forced by tides specified along the open boundaries using harmonic tide predictions (Flater 1996), freshwater inflow, and wind and heat flux at the water surface. The meteorological parameters for 2007 were obtained from the Weather Forecasting Research (WRF) model reanalysis data generated by the University of Washington. Available WRF data were on a coarse 12-km grid and required a 20% reduction of net heat flux to account for different albedo over land vs. water, as part of calibration of water surface temperatures. Temperature and salinity profiles along the open boundaries were specified based on monthly observations taken by the Department of Fisheries and Oceans, Canada in 2007. The model includes 19 gaged major rivers, 45 nonpoint source loads, and 99 wastewater treatment plant discharges. The nonpoint source and watershed stream flow were estimated through a combination of measured stream flow data from 2007 and hydrologic modeling analysis conducted by Washington State Department of Ecology (hereafter Ecology; Mohamedali et al. 2011).

Figure 2 shows a comparison of measured and predicted tides, currents, salinity, and temperature at the marine water quality monitoring station near Seattle (PSB003) as an example. As part of hydrodynamic model QA/QC, similar time series plots were generated at nine other monitoring stations in Puget Sound. Error statistics were computed as part of model validation and are listed in Table 1.

Use of PSGB model output in eelgrass model

The PSGB model results for 2007 were made available for all nodes in the computational mesh. Results were archived at six-hour intervals and by layer. There were ten PSGB layers in total. Only the surface layer results were used by the eelgrass model, though other layers could potentially be used. In the shallow regions that we are considering as locations for eelgrass (see *Creating Nodal Stations* below), water amongst these layers in the hydrodynamic model is generally well-mixed, as opposed to deeper parts of the Sound where stratification is likely to occur. Thus, use of different layers should not have significant impact on the results. The PSGB model results are archived using Matlab 7.3 file format. This format allows for targeted reading segments of these large files.

A short Matlab script was written that extracted and stored the PSGB model results following estimated fields from the archived results. Only the following fields produced by the PSGB model were used by the eelgrass model: water surface elevation, water temperature, and salinity. Once data was extracted, linear interpolation was used to reconstruct hourly time steps from the six hour intervals. The type of interpolation (e.g. linear vs. cubic) did not have measurable effects on model outcome.

Water surface elevation

The water surface elevation estimates were extracted for use in estimation of light levels at canopy depths (see *Light* and *Attenuation* sections below). These elevations are provided as elevations in meter NAVD88.

Water Temperature

The water temperature estimates were extracted for use in estimation of productivity and respiration rates. Water temperatures are provided in degree C.

Salinity

Salinity estimates were extracted for use in estimation of the effects of decreases in salinity on photosynthesis and are provided in ppt.

Creating Nodal Stations

The PSGB model has 9,013 nodes where the model estimates of hydrographic and water quality information is created. We determined 5,076 of these nodes were close enough to the shoreline to either be directly located over potential eelgrass habitat or adjacent but slightly offshore to potential habitat to warrant application to the eelgrass model. Only this 5,076 node subset was further considered in the eelgrass model. A second Matlab script and a function were created to read the nodal time history of the selected PSGB model parameters (water surface elevation, temperature, salinity) and archive these results as a station file identified by PSGB node index and geographical position. These station archive results were stored in a Matlab binary file for 5,076 locations individually and at the six-hour archive interval of the PSGB model. The approach allows for rapid evaluation of single or small number of locations to be evaluated by the eelgrass model without requiring additional runs of the circulation and transport model.

Eelgrass biomass model

The eelgrass biomass model was based on a lineage of seagrass models including Burd and Dunton (2001) modeling the seagrass *Halodule wrightii* and Eldridge et al. (2004) modeling *Thalassia testudinum*, both in Laguna Madre, Texas. These models focus on the carbon stored in seagrass per a unit area, rather than the dynamics of individual plants, shoots or leaves. The Eldridge et al. (2004) model has been adapted for *Z. marina* in Yaquina Bay, OR, but that work was never completed (Kaldy and Eldridge, 2006). We began with the model as described in the unpublished report and updated the model with data from Puget Sound. When possible, we have further developed the model to accommodate stressors experienced in Puget Sound and the observed range of environmental variability.

We represent eelgrass biomass (in terms of carbon) for aboveground (C_a) and belowground (C_b) compartments with discrete-time difference equations:

$$C_{a,t+1} = C_{a,t} + \Delta t \left[(1-\tau) P(I_z, T, S) C_{a,t} \left(1 - \frac{C_{a,t}}{\kappa} \right) - R_a(T) C_{a,t} - M_a C_{a,t} \right] \qquad (1)$$

$$C_{b,t+1} = C_{b,t} + \Delta t \left[(\tau - \delta) P(I_z, T, S) C_{a,t} \left(1 - \frac{C_{a,t}}{\kappa} \right) - R_b(T) C_{b,t} - M_b C_{b,t} \right] \qquad (2)$$

where τ is the translocation of carbon from aboveground compartments (shoots and leaves) to belowground compartments (roots and rhizomes), δ is exudation of carbon from roots, P is photosynthetic production as a function of light (I), temperature (T), and salinity (S), κ is a density dependence parameter, R is the respiration rate as a function of temperature, and M is the loss rate of biomass to processes other than respiration, such as leaf loss. Subscripts a and b are used to refer to aboveground and belowground model components, respectively. Each of these variables and parameters are further explained in the following sections. We run the model as a difference equation updated on an hourly time step ($\Delta t = 1$).

Light
We use a multistep process to calculate light at eelgrass canopy level for a specified depth. The hourly light levels used by the eelgrass model are consistent with those used by the water quality model; these are based on scaling the daily total shortwave radiation as estimated by the University of Washington's Weather Research Forecasting model to an hourly basis. Instantaneous surface light level calculations were based on time since sunrise, day length, and daily total shortwave radiation, following established methods accounting for the angle of the sun (Kirk 1994). The time for sunrise and sunset were obtained online from UNSO (http://aa.usno.navy.mil/data/docs/RS_OneYear.php).

Light levels just below the water surface are reduced from the instantaneous surface light levels due to reflection, also calculated according to established methods (e.g., Kirk 1994). On an hourly basis, we computer the incident angle and fraction of light reflected at the water surface. The incident angle is computed based on declination angle, latitude and time of day. The declination angle is computed based on the day of year and latitude. For the purposes of this study, the latitude for all model locations was set to 47° 36' N. Once the fraction of light reflected from the water surface is calculated, we can use the remaining fraction to determine I_s, the irradiance just below the surface. These light levels were applied

homogenously to all model nodes. Node-specific conditions were then used to estimate attenuated light levels as described in the following section.

We calculated light at canopy level (I_z) using the following equation:

$$I_{z,n,i} = I_s e^{-K_{PAR(n,i)}z}$$
(3)

where I_s is photosynthetically active radiation (PAR) just below the water surface, z is canopy depth in meters, and K_{PAR} is the attenuation coefficient calculated for region *n* and month *i,* as described below.

Attenuation

Light attenuation, one measure of turbidity, is one of the primary controlling factors that determines the presence and growth of eelgrass in Puget Sound waters and elsewhere. Attenuation of light in the water column is a function of dissolved and particulate constituents. It can vary greatly depending on the location and event-driven, seasonal, or annual variability of biotic and abiotic components. These components both absorb or scatter light, effectively reducing the amount of PAR available for plant growth. The primary optically active components include chlorophyll (phytoplankton), dissolved organic matter (DOM) and total suspended sediments (TSS) including detritus. The light attenuation coefficient (K_{PAR}) measures the collective absorption and scattering properties of each component and is proportional to their concentrations such that:

$$K_{PAR} = K_W + K_{DOM}[DOM] + K_{CHL}[CHL] + K_{TSS}[TSS]$$
(4)

where *K* represents the specific attenuation coefficient for each constituent, w is pure water, DOM is dissolved organic matter, CHL is chlorophyll, and TSS is total suspended sediments. Attenuation due to pure water is negligible in coastal waters that are largely influenced by other biotic and abiotic materials. The PSGB models components of DOM and chlorophyll in the water column, but does not model TSS. As TSS can be a significant contributor of turbidity in potential eelgrass habitat, especially near river deltas (Loos and Costa 2010), we needed to obtain estimates of light attenuation that include TSS as well as dissolved organic matter and chlorophyll.

Ideally, light attenuation data collected from representative areas of Puget Sound over time would be the most relevant input for the eelgrass biomass model. However, there is generally a paucity of light attenuation information that has been collected for this region. Hence, our approach was to use previously acquired Secchi depth data from areas around Puget Sound to develop spatially and seasonally relevant approximations of light for the eelgrass biomass model. The Secchi depth, z_{SD}, is an easily collected measure of water clarity/turbidity that relies on estimating the distance of a Secchi disk disappearance in the water column (Davies-Colley et al. 1993). Although less precise than measurements with optical sensors, it is a useful measure of visual water clarity that has been related empirically to optical measurements such as light attenuation (Kirk 1994). Since Secchi depth data were available to a much greater extent throughout Puget Sound over time, we used these data to develop a relationship with previously acquired K_{PAR} data from a specific location in the Sound.

In a previous study, we collected light attenuation and Secchi depth data at two locations in Sequim Bay between June 2009 and August 2010 on a weekly basis that encompassed a variety of optical conditions with respect to suspended sediments, phytoplankton, and organic matter content (Woodruff, unpublished). Underwater PAR data were collected using a LiCOR 4π quantum irradiance sensor at various depths and K_{PAR} was then calculated using the following equation based on Beer's Law:

K_{PAR} = -ln(I_2/I_1)/d   (5)

where K_{PAR} is the attenuation coefficient (m^{-1}), I_x is irradiance measured at distance x in the water column ($\mu mol\ m^{-2}\ s^{-1}$) and I_y is irradiance measured at distance y in the water column ($\mu mol\ m^{-2}\ s^{-1}$), and d is the vertical distance between I_x and I_y. K_{PAR} data were regressed against the Secchi depth, $z_{SD,}$ to develop an empirical relationship between the two (r^2 = 0.78). We then applied this equation to Secchi depth data collected in other parts of Puget Sound to calculate an approximate K_{PAR} for various locations.

We used a long-term Secchi depth dataset collected by Ecology's Marine Water Quality Monitoring program(http://www.ecy.wa.gov/programs/eap/mar_wat/data.html) to calculate K_{PAR} for specific regions of interest. Ecology maintains a suite of sites that are sampled on a monthly basis as either core and rotating sites. For our initial assessments, we used Secchi data from sites around Puget Sound that were selected to represent a regional water body or a specific area of interest/concern. The data used encompassed the years between 1999 and 2009 and were collected on a monthly basis, weather permitting. We summarized available data and used monthly mean K_{PAR} values for individual regions. The sites and data included are listed in Table 2, with a map of regions in Figure 3. Attenuation coefficients generally ranged between approximately 0.05 and 0.7 m^{-1}.

K_{PAR} data were then incorporated into the eelgrass biomass model to determine the light available at a specified depth. We calculated light at canopy level (I_z) using the following equation:

$$I_z = I_s e^{-K_{PAR}z}$$ (6)

where I_s is PAR just below the water surface and z is canopy depth in meters. Canopy

Photosynthesis
We model gross photosynthesis as a function of light and temperature, mediated by salinity. Previously published models (Burd and Dunton 2001, Eldridge et al. 2004) include the effect of temperature on photosynthesis as an exponentially increasing function ($e^{k\Delta T}$). Data from Sequim Bay, WA (Thom et al. 2008, unpublished) suggest that the maximum gross photosynthesis rate of locally adapted eelgrass increases with temperature only to a point, and then decreases. Accordingly, we fit the experimental data for gross primary production to several models to determine the best relationship of photosynthesis to light and temperature for Puget Sound, as described below.

We utilized net productivity and respiration data developed during experiments at the Marine Sciences Laboratory, located at the mouth of Sequim Bay, WA. Net productivity, using dissolved oxygen flux, was generally measured in short-term (e.g., 2-4 hours) incubations of healthy leaf sections contained in clear glass jars (Thom et al. 2008). The jars were submersed in shallow trays filled with running seawater from

the mouth of Sequim Bay, and exposed to ambient sunlight. We routinely employed five replicate bottles containing eelgrass in the experiments, along with five replicate control (water only) bottles. Light (PPFD) and water temperature were recorded periodically during the experiments. Following a similar procedure, we also measured respiration rates by excluding all light reaching the jars. Because respiration rates are generally low, we incubated the jars for longer periods (ca., 4-8 hours) in order to obtain reliable oxygen change measurements. Finally, to evaluate the effect of temperature on net productivity and respiration, we conducted an experiment involving manipulated water temperatures relative to ambient conditions (i.e., ambient, cold and hot) by incubating the jars in water baths kept at the various temperatures.

From the experimental data for net primary production we estimated gross primary production based upon the regression of respiration to temperature (see *Respiration*). We fit the experimental data for gross primary production to several models, using either the Jassby-Platt photosynthesis-irradiance (P-I) curve (Jassby and Platt 1976, Burd and Dunton 2001) or the Smith-Talling P-I curve (Eldridge et al. 2004). We tested models in which the maximum photosynthesis rate (P_{max}) varied either exponentially or quadratically with temperature. We also included models where the parameter α, which determines the intial slope in the Smith-Talling formulation, or I_k, which determines the saturation point in the Jassby-Platt formulation, are allowed to vary linearly with temperature and models where they are held constant.

We fit the photosynthesis models to the mean photosysnthesis rate for each treatment using MATLAB's surface fitting tool (MATLAB and Curve Fitting Toolbox Release 2012a). Model fit statistics are provided in Table 3. We also calculated the Akaike Information Criteria corrected for small sample sizes (AIC_c) to aid in selection of the best-fitting and most parsimonious model. Models with quadratic temperature-P_{max} relationships fit the data much better (R^2 values between 0.31 and 0.33) than the exponential relationships (R^2 values of 0.13 and 0.15). The fits to the two P-I functional forms were very similar, with the Smith-Talling function performing slightly better than the Jassby-Platt formulation. The similarity is not surprising as there was limited availability of data at the lower light levels in this experiment to use to determine the shape of the curves. There was especially limited experimental data at low light with higher temperatures; consequently there was high uncertainty in the fits of the two shape parameters α and I_k. In the models where these parameters varied with temperature, the slopes were near 0 with 0 included in the 95% confidence intervals for those parameters. Given this uncertainty and the AIC results which suggest that the gains to fit from including temperature dependence upon shape do not outweigh the cost of an additional parameter, we decided to hold the shape parameters constant.

The two P-I formulations tested had similar fits to the data, but the Jassby-Platt formulation was better behaved at the edges of the model domain. We tried both formulations in the productivity model and found, at most, 0.5% differences in model outputs at particular sites and usually much less. We also tested the model with the Jassby-Platt formulation with a constant or time dependent I_k, and found differences in final biomass of up to 2% in some localized areas. In general, the difference between the final biomass predicted by the two models is <0.5%. The similarity of output in both of these cases suggests that the differences between these models will not affect the relative ranking of site suitability.

Based upon these considerations, we model photosynthesis as a function of light and temperature using the Jassby-Platt formulation where P_{max} is a function of temperature but I_k is held constant:

$$P(I,T) = P_{max}(T)tanh\left(\frac{I_z}{I_k}\right) \tag{7}$$

where P_{max} is the maximum photosynthesis rate, I_z is PAR at canopy, and I_k is the saturation parameter. P_{max} is a quadratic function of temperature:

$$P_{\max(t)} = \beta_{p2}T_t^2 + \beta_{p1}T_t + \beta_{p0} \tag{8}$$

The dependence of gross primary production (GPP) upon temperature and light is shown in (Figure 4; R^2 = 0.31).

Photosynthesis has been shown to decline when salinity decreases below normal seawater concentrations, as would be observed near river mouths. We use data from salinity reduction experiments (Mullin and Thom, unpublished) to fit a linear model (Figure 5; R^2 = 0.82) of the proportional reduction in gross photosynthesis as salinity (S_t) decreases from 30 ppt:

$$S_t = \beta_{s1}T_t + \beta_{s0} \tag{9}$$

This adjustment is applied after GPP is calculated for each time step.

Density dependence
Photosynthetic production is also limited by density dependence, particularly self-shading. This is represented by the term $\left(1 - \frac{C_{a,t}}{\kappa}\right)$. The strength of density dependence for a particular level of aboveground biomass depends upon the density dependence parameter κ. While κ is sometimes referred to as the carrying capacity, and functionally is related to the carrying capacity in a general logistic equation, it should be noted that in our model, equilibrium biomass will always be below (in some cases, well below) κ due to the concurrent effects of respiration, mortality, and other limiting factors upon photosynthetic production.

Respiration
We model respiration as a function of temperature. Respiration is traditionally modeled as an exponential function of temperature, but data from Thom (unpublished; described in *Photosynthesis* above) showed a linear increase in respiration with increasing temperature (Figure 6; R^2 = 0.85). Accordingly, when using the Puget Sound data we use the following function to model respiration:

$$R_{a,t} = \beta_{r1}T_t + \beta_{r0} \tag{10}$$

The available data does not include data on belowground respiration. To model respiration belowground, we use the same formulation for aboveground multiplied by the ratio of belowground respiration to aboveground respiration used in the EPA model (Kaldy and Eldridge 2006).

Translocation and exudation

We assume that a constant proportion of carbon τ fixed by photosynthesis during every time step is transported to the roots and rhizomes of the plant. Once in the belowground compartment, another proportion δ of aboveground production is lost through exudation from the roots.

Mortality

Mortality in the biomass model includes the loss of carbon in aboveground or belowground compartments due to breakage or grazing. Consequently, mortality is higher aboveground than belowground due to greater exposure. Currently, we model mortality as a constant loss rate. We lack data on mortality, so estimated the parameter based on the rate used in Kaldy and Eldridge (2006) but adjusted for the overall lower rates of productivity in our model. While the lack of information on mortality is a data gap in the model, note that changes to this rate will not affect *relative* predictions of the model, as we are using it in this application, because eelgrass in all areas would be affected equally by changes.

Nutrients

While nutrient limitation is included in some eelgrass biomass models, we did not include them in our model due to limited evidence of nutrient limitations in Puget Sound.

Most seagrass species can take up inorganic nutrients both through roots and leaves. Numerous experiments in which nitrogen and/or phosphorus have been artificially added to the sediments have resulted in enhanced growth of seagrasses (Orth 1977, Short 1987, Hemminga and Duarte 2000, Romero et al. 2006). However, there also have been many fertilization experiments that showed no response (Romero et al. 2006). In these, it is assumed that nutrients were not limiting growth. Further, seagrasses have the ability to reclaim nitrogen from old tissues, thereby supplementing their nutrient requirements especially when nutrients may be in low concentrations (e.g., Pedersen and Borum 1992).

Williams and Ruckelshaus (1993) conducted water column and sediment enrichment experiments in the extensive eelgrass meadows at Padilla Bay. They found a slight enhancement of growth in April experiments, but not those conducted in August. They also recorded greater epiphyte loads on the leaves in response to higher water column nutrients. Suppression of eelgrass growth by greater epiphyte loads (i.e., that shaded eelgrass leaves, and competed for nutrients) was partially mitigated by an epiphytic grazing isopod. Based on this work, they concluded that consideration of sediment nitrogen, epiphytes, and herbivores alone is unlikely to yield a predictable understanding of the control of eelgrass primary productivity in nature. Although stimulation of growth was recorded in April, it appeared to us that the mean concentrations of ammonia measured in unfertilized sediments were well above those required to saturate eelgrass growth.

Eelgrass growth was measured over a six-week period at our laboratory in six natural sediments treatments containing various levels of organic matter (Thom et al. 2001). Growth rate was highest in the fine organic sediments collected from two marsh channels, and the eelgrass meadow. Growth rates were about 30% slower in coarse sand and sand/gravel mixtures with low organic content. Growth rates in sediment containing essentially no organic matter (i.e., gravel/cobble mix) were ~70% lower than the highest rates.

Zimmerman et al. (1987) evaluated nitrogen limitation on *Z. marina* growth and concluded that such limitation was rare. Their research indicated that *Z. marina* could grow at normal rates for at least 30 days without an external supply of nitrogen. They support this finding by a determination that about seven days of exposure of external sources would be needed to replenish internal nitrogen reserves.

Based on these studies we conclude that nutrient limitation may be rare or short-lived in areas where eelgrass is abundant in Puget Sound. Thus our present model considers there to be no nutrient limitation. However, we do recommend that in nearshore areas where water column nutrients can reach very low levels especially in spring (e.g., Thom and Albright 1990) and sediment is generally low in organic matter content, that further evaluations (e.g., sediment sampling) may be warranted regarding the potential for nutrient limitation to suppress the colonization and spread of eelgrass.

Parameterization

We parameterized the model with data for Puget Sound from Thom et al. (2008 and unpublished) in Sequim Bay, WA, when possible as described above. This was done for parameters involved in calculations of photosynthetic production and respiration. For other parameters, we used values from the EPA study (Kaldy and Eldridge 2006). Parameter values and units are listed in Table 4.

Simulations

We ran two main types of simulations: single site (or comparisons of several sites) and spatially extensive simulations. In both cases we used PSGB model output at the 5,076 nearshore nodes as inputs to model eelgrass biomass at that location at a specified depth. In the case of spatially extensive simulations, we merely repeated this process over a part or all of the selected nodes. The model was run independently at each node; that is, there are no effect of eelgrass growing at one location on eelgrass growing at nearby locations.

Comparison of model output with DNR monitoring data

We compared model outputs with DNR monitoring data to assess the quality of model predictions. To do this, we identified model nodes that were in, or just adjacent to, sites that had been surveyed by DNR during the years 2000-2010. Percent cover is not directly estimated through the monitoring program, so we estimated it by calculating estimates of percent cover from DNR area estimates divided by the area of a site, with site area defined as the area of the sampled location between 0m and -5.4m depth (MLLW; -5.4m was chosen as a standard maximum depth for eelgrass to allow for consistency in area measurements across sites.) If there were multiple years of monitoring data, we used the average of the percent cover estimate for all years surveyed. We then converted percent cover to proportions between 0 and 1 to represent an index of site suitability for eelgrass. It was possible for this method to estimate more than 100% cover in some cases where eelgrass grew at depths greater than -5.4m. In these cases, which occurred at less than 2% of sites, we capped the percent cover estimates at 100% so that, when indexed, the suitability measures would be distributed more evenly across the range from 0 to 1. We also scaled predictions from the eelgrass biomass model for biomass at -3m NAVD88 (chosen as a representative depth where biomass is driven by all factors rather than strongly determined by either light availability or temperature) at the end of the simulation year between 0 and 1 to facilitate

comparisons. The lowest predicted biomass is set to 0, the highest predicted biomass is set to 1 and all other values are standardized to this scale.

Results

Eelgrass dynamics at a single site

Figure 7 contains hourly output from the eelgrass model at a site located in Sequim Bay, WA. Photosynthetically active radiation at the canopy level is driven by light availability at the surface, determined by time of year, day, and cloudiness. Light passing through the surface of the water is attenuated through a variable depth of water, dependent upon tides. Monthly attenuation coefficients range between 0.06 and 0.38. Water temperature and salinity are direct inputs from the PSGB model for this location. This site in Sequim Bay is a relatively cool-water site without significant freshwater input.

Photosynthetic production is represented both as hourly data (blue line) and daily average hourly rates (green line) in Figure 7. Hourly photosynthesis rates vary with the daily cycle of light availability, but the daily average shows the effects of seasonal patterns in light availability and water temperature. Respiration is a linear function of temperature, and thus predicted respiration rates correlate directly to temperature. The hourly growth rate (change in biomass) is positive during the day when photosynthesis is occurring and negative at night. Overall growth declines during warmer summer months when photosynthesis is insufficient to compensate for the temperature-induced increase in respiration. Consequently, aboveground biomass peaks during the early summer, remains roughly constant through the summer, and declines somewhat in the fall and winter. These changes in biomass during the course of the year are subtle, and while they do reflect much of the seasonal pattern of biomass changes observed in the field, they do not represent the typical magnitude of such changes. Under the current parameter set, aboveground biomass is expected to increase very slightly over the course of a year at this location.

Comparison of two sites with contrasting conditions

Figure 8 contains model inputs and outputs from two sites: Sequim Bay (thick lines) and Hood Canal near the Great Bend (thin lines). To facilitate comparison, we show mean daily hourly rates for PAR, photosynthetic production, and growth rates.

For most of the year, attenuation is higher at the Hood Canal site, leading to lower intensities of light reaching -3m NAVD88 in Hood Canal compared to Sequim Bay. Water temperatures are also higher during most of the year, by as much as 10°C during summer months. Salinity is also lower and more variable at the Hood Canal site. Respiration is notably increased for Hood Canal eelgrass during the summer months compared to Sequim Bay due to higher temperatures. Similarly, gross photosynthetic production is lower in Hood Canal both during late summer when temperatures are high and during winter months when attenuation is high and less light is available. As a result, the growth rate is negative for much of the year in the Hood Canal site, and most negative in the summer months. This leads to a decrease in biomass both above- and below-ground for the Hood Canal site. Under the

current parameter set, which predicts general stability or a slight increase in aboveground eelgrass in Sequim Bay, eelgrass at the Hood Canal site would be expected to decline.

Model predictions throughout Puget Sound

Figures 9-11 show mean and extreme eelgrass biomass model inputs for water temperature and salinity (output from PSGB model) and attenuation coefficients (calculated from Secchi depths as described above.) Mean water temperatures over one year are highest in Hood Canal, with warm water also predicted for a number of areas in central Puget Sound and north of the San Juan Islands. The coolest mean water temperatures are generally found in embayments, along the Strait of Juan de Fuca and along the northern mainland and northern Whidbey Island. Maximum water temperature follows a similar pattern, with maximum water temperatures predicted for Hood Canal much higher than in other regions and coolest maximum temperatures along the Olympic Peninsula into Admiralty Inlet.

Modeled salinity patterns (Figure 9) are driven by the location and size of rivers. Mean salinity is similar throughout the Sound except for immediately at the large river deltas, particularly along the eastern edge of the Sound near the Skagit and Snohomish river deltas. The map of minimum salinity reflects large freshwater inputs during storm events creating areas of low salinity in river deltas and surrounding bays during portions of the year. Areas rarely modeled to experience low salinity include northern Hood Canal, central portions of South Sound, and bays such as Sequim, Discovery, and Liberty Bays without significant freshwater drainages.

Similarly, attenuation coefficients are typically highest in both their mean and maximum values over the course of a year (Figure 11) at the deltas of large rivers (e.g., Skagit, Nooksack, Nisqually) and areas of low circulation (South Sound, Liberty Bay, Penn Cove).

These spatial patterns of environmental quality are reflected in the eelgrass biomass model predictions for single depths (NAVD88 elevations; Figure 12-14). These figures represent the biomass of eelgrass after a year if grown at the specified depth at each location. (Note that running the model at a specified depth changes the water level above the canopy and therefore the amount of PAR reaching the eelgrass canopy, but does not affect the other forcing variables of temperature or salinity.) While these maps do not reflect the actual physical area likely to be occupied by eelgrass based on bathymetry and other constraints (see technical memo for Task 5), they allow for an overview of eelgrass growth potential throughout different regions of Puget Sound based upon the spatially variable forcing factors plotted in Figures 6-8. Across modeled depths, the greatest potential for eelgrass growth is predicted for the Olympic coast through Admiralty Inlet, Padilla Bay, and areas of central and southern Puget Sound. Areas of lowest potential include Hood Canal, particularly southern Hood Canal, areas on the north side of the San Juan Islands, and the large river deltas. At the 1m depth, distribution is mainly driven by salinity and temperature, but at 5m depths eelgrass dynamics are determined primarily by light attenuation, as would be expected given the primary role of light in determining lower depth limits. Note that some factors affecting eelgrass at shallow depths (e.g. desiccation) will be taken into account during GIS post-processing and are not currently incorporated into this model.

The scatter plots in Figure 15 show the dependence of biomass upon the forcing variables of water temperature, salinity, and attenuation. Each point in the scatter plot represents the final biomass at a particular site (i.e., a single point in Figure 13.) Biomass generally declines with increases in mean and minimum water temperature, though there is large variability in model outcome around mean temperatures between 9.5°C and 11°C and maximum temperatures between 15-17°C, at which points other factors become more important. Similarly, biomass increases with salinity, with mean salinity is more predictive than minimum salinity. Again, larger variability in outcomes are seen at high salinities where other factors become limiting. Likewise biomass decreases somewhat with increasing mean and maximum attenuation.

Comparison of model output with DNR monitoring data

In Figures 16 and 17 we compare biomass predictions against percent cover estimates in areas where eelgrass surveys have been conducted. To facilitate comparisons, we standardized biomass and percent cover metrics to a 0 to 1 scale where 0 is the lowest predicted final biomass and 1 is the highest, and percent cover is converted to proportional cover, also from 0 (low) to 1 (high). Note that percent cover was not directly recorded by the eelgrass monitoring program, and direct comparisons of percent cover and biomass may be misleading, but the data nonetheless provides for a general (though not statistically rigorous) comparison of site suitability predicted by the model with site suitability as indicated by the extent eelgrass cover. In the northern half of the Sound (Figure 16), the model does fairly well at predicting low eelgrass potential in the Skagit, Snohomish, and Nooksack deltas as well as the north San Juan Islands, higher eelgrass potential between Dungeness Bay and Sequim Bay, Padilla Bay, and moderate potential in areas of Central Sound. The greatest contrast between model predictions and results are near the southern San Juan Islands, the western edge of Whidbey Island and some parts of Admiralty Inlet and along the Strait.

In the lower half of the Sound (Figure 17), the model is relatively consistent at predicting moderate eelgrass potential in areas of Hood Canal that are predicted to be poor eelgrass habitat and areas of central Puget Sound that are observed to have moderate levels of percent cover. The largest discrepancies are in South Sound, where the biomass model does not account for limitation to the upper range of eelgrass due to desiccation from high tidal ranges (this will be accounted for during GIS post-processing of model results) and some more inland areas of Central Sound (e.g. Liberty Bay) where the model predicts higher potential but eelgrass is generally not found.

The model is significantly better than random chance (p< 0.0001) at predicting percent cover. However, the variability is very high, with an R^2 of 0.06.

Discussion

Application of the eelgrass biomass model to Puget Sound

We made several changes to the model developed by EPA for *Z. marina* in order to apply the model to Puget Sound. The most notable changes were to the effects of temperature and salinity on net productivity.

Temperature and metabolism relationships

The seagrass biomass models (Burd and Dunton 2001, Eldridge et al. 2004) that were the starting point for this model included the same exponential dependence of respiration and photosynthesis upon temperature. This model suggesting that both photosynthesis and respiration would both occur at increasingly higher rates as temperature increased, and therefore higher water temperatures were most conducive to eelgrass growth. While this may be true for environmentally likely temperature ranges for eelgrass species adapted to higher temperatures, experimental evidence from Puget Sound (Thom et al. in revision) and other Pacific Northwest sites (Thom et al. 2003) suggests that maximum net photosynthesis rates when light is not limiting reaches a maximum at moderate temperature ranges (~ 8˚C) and then declines as temperature increases further. The observed decline in productivity is not simply due to a relatively faster increase in respiration as compared to gross photosynthesis, but also a decline in gross photosynthesis at increased temperatures (Figure 4). In addition, observed respiration rates were best fit to a linearly increasing model rather than an exponentially increasing model (Figure 6). Therefore we used a linear function of respiration with temperature, but a quadratic relationship of gross photosynthesis with temperature to reflect the declines in productivity observed for eelgrass adapted to cool water in Puget Sound when exposed to warmer waters. While there is the possibility for local adaption to warmer water, e.g. for eelgrass populations in southern Hood Canal, we lack data specific to these situations and do not currently include local adaptation in this model.

Salinity and photosynthesis

Previous models for eelgrass biomass have generally not included effects of salinity on photosynthesis, or included it in very limited ways. We incorporated a functional dependence of gross photosynthesis on salinity, where decreases in salinity cause a linear decrease in photosynthetic production as suggested by experimental data (Mullin and Thom, unpublished data). This allows the model to better predict eelgrass growth near large river deltas, in which eelgrass growth is limited by freshwater input.

Comparison with monitoring data

The model shows mixed results when potential for growth is compared with eelgrass monitoring data. Such an exercise is not a formal model validation for several reasons. First, neither biomass nor percent cover are measured by the monitoring program, and our conversion of available data to percent cover introduces significant uncertainty. Secondly, the current eelgrass biomass model is deterministic, without error estimates in parameters and predictions that would allow for statistics of model fit to be calculated. Third, locations that are suitable for eelgrass but where eelgrass was not observed (as this project is intended to identify) will appear as large errors in our predictions, but are not actually errors in the model. These factors preclude a statistically rigorous validation process and make it difficult to meaningfully quantify model accuracy. However, this comparison does allow us to assess general patterns in the relationship of the biomass model to actual eelgrass distributions.

The R^2 of a linear regression of predicted growth potential to observed percent cover is low, at 0.06, though that is an improvement over the original model (before adapting the model to Puget Sound) which resulted in an R^2 of 0.01.

Differences in model predictions from monitoring data can result if any or all of the following are true:

- Biomass model inputs of water temperature and salinity provided by the hydrodynamic model or light attenuation developed from marine water quality monitoring do not accurately reflect conditions experienced by eelgrass during and before monitoring.
- The model structure has errors; i.e. the functional relationships do not represent how Z. marina in Puget Sound responds to environmental factors, or mechanisms are missing. (Note: some mechanisms can be accounted for in GIS post-processing that are not included in the model, e.g. filtering results for areas of unsuitable substrate.)
- The model structure is essentially correct, but the parameterization of the model are incorrect, due to insufficient data or data that does not accurately represent the physiology of eelgrass throughout Puget Sound.
- Neither biomass nor percent cover are directly measured by the monitoring program, and our conversion of available data to percent cover introduces some uncertainty. Areas of low percent cover of healthy eelgrass, or higher cover of unhealthy eelgrass, would be inaccurately compared to our model. There is also a degree of observation error inherent to the monitoring process.
- Locations that are suitable for eelgrass, but where eelgrass is not found due to recruitment limitation or past disturbance, will count as error in the model validation process when in fact the habitat may be suitable for eelgrass restoration.

All of these factors potentially contribute to error in model predictions, and given the limited availability of environmental, physiological, and monitoring data, are difficult to disentangle at this time. The effects of these factors should be considered when applying the model, such as whether local adaption or recruitment limitation is likely at a particular site.

In the course of model development, improvements in the model such as the addition of salinity effects and more specific light attenuation data improved the model predictions in areas such as Skagit Bay. In other areas we still observe systematic differences. For example, the model is pessimistic about potential for eelgrass in Hood Canal, yet there are some areas of relatively high eelgrass cover. In this case, eelgrass in Hood Canal may have adapted to warmer water, but since the model was parameterized with data from eelgrass adapted to cooler water, it may underestimate the ability of eelgrass to successfully grow in Hood Canal. It is also possible in such cases that our driving variables of water temperature or turbidity may not be accurate as applied, thus creating overly pessimistic predictions.

Throughout Whidbey Basin and areas of central Puget Sound, the model predicts moderate to high potential for eelgrass, yet monitoring data presents a range of results from eelgrass absence to abundance. The disparity may be due to local adaptations or shortcomings in functional responses to driving variables or driving variables themselves, as just described, or contributions of factors not included in the model at all. Localized stressors such as wave energy, human activity, or problems with water quality, sediments, and/or macroalgal blooms (Thom et al. 2011) may affect eelgrass distribution in some areas in ways that the model cannot predict. Some of these potential limitations are described in the following section.

Limitations and caveats

There are a range of limitations and caveats for the current version of the eelgrass biomass model. Some we have been able to partially address with available data, others are not currently included in the biomass model but are incorporated into further GIS processing of eelgrass information and model projections for site selection (see Task 5 memo), and others we have not yet been able to address.

Turbidity and attenuation

As the PSGB model does not currently include suspended sediments, we were unable to use spatially modeled turbidity information as an input to the eelgrass biomass model. Light attenuation, however, including that caused by suspended sediments, is as significant driver of spatial variability in eelgrass habitat quality throughout Puget Sound. We were able to use information from the Puget Sound Marine Water Quality Monitoring program to calculate turbidity for various regions using Secchi depth data. Currently we include data from 15 monitoring stations to apply to regions throughout the Sound, including major river deltas and embayments with low circulation. Limitations remain for this data, however, including the general lack of nearshore turbidity data and overall spatial and temporal resolution of data. The number of water quality monitoring sites is limited, usually located in deeper water, and not all sites have sufficient years of data to reflect the variability possible in turbidity during and across years. The monthly observation frequency is also not high enough to describe short-term variability, though very short-term variability will likely be averaged out during the eelgrass production process. Due to the nature of collecting data through Secchi depths, it is possible that measurements may not be taken during the worst conditions. However, the monitoring program appears to be consistent over time and any bias introduced due to weather conditions is likely small relative to other data gaps.

Desiccation

Desiccation of eelgrass growing at shallow depths due to extended exposure to air is a significant limiting factor to eelgrass depth distributions, particularly in areas with high tidal amplitude such as South Sound. While we did not include desiccation in the model directly, we are using upper depth limits to predict the actual depth range and area through GIS processing of model outputs as will be described in the corresponding technical memorandum.

Substrate and energy

The eelgrass biomass model does not include consideration of substrate and wave energy in predicting eelgrass growth potential. Substrate will have considerable effects on eelgrass distribution, and we may be able to incorporate some of these effects through GIS processing (e.g., to remove sites with rocky substrate from consideration) if data is available. Similarly it may be possible to filter sites based upon wave energy according to estimates of fetch or the presence of armoring. It is conceivable that wave energy could be included as a driving factor for eelgrass mortality in the biomass model, but that would likely require considerable effort in deriving the correct inputs and functional relationships.

Seasonality

The seasonal patterns generally observed in eelgrass biomass are not highly evident in the model results. While there is a seasonal pattern of increased net productivity during spring, increased

respiration in summer, and low photosynthesis and respiration in winter, these patterns are not as strong as would be seen in the field. There are multiple potential reasons for this. One possibility is that our model of gross primary production underestimates the growth potential in the spring. Another is that seasonal changes in mortality—e.g. increased losses of leaves and entire plants during winter storm events—are not represented in our constant mortality function. A third possibility is that the carbohydrate transport from belowground to aboveground during winter or early spring, which helps the plant recover from higher mortality and lower production during the winter, is not currently included in the model (see next section). Changes to these functions would likely increase the seasonal patterns in the biomass predictions; however, for the most part, we lack sufficient data to develop these functions further at this time.

Carbohydrate transport

The movement of carbohydrates amongst eelgrass above- (leaves) and belowground (roots and rhizomes) compartments can be a significant factor in the long term survival of eelgrass in higher latitudes where photosynthesis is greatly reduced during winter months. Previous models such as presented by Burd and Dunton (2001) have included translocation of carbohydrates produced in the shoots to roots and rhizomes, as the sources of carbohydrates for underground biomass. That model, however, does not allow for movement of carbohydrates from belowground to aboveground. Other applications of the model (Eldridge et al. 2004) do not explicitly model the belowground compartment. While use of belowground carbohydrates may be less important for eelgrass species or populations in lower latitudes (i.e., Texas), storage of carbohydrates in the roots to support plants during winter may be more critical in Puget Sound and need to be explicitly modeled.

Our model does not currently include translocation of carbohydrates from belowground to aboveground pending identification of appropriate triggers and functional forms for storage of carbohydrates and use of stored carbohydrates, which we could not complete in the scope of this project. Modeled eelgrass dynamics over the course of the year do not currently demonstrate reductions in biomass during winter months as are typically observed in Puget Sound. As this reduction is a likely trigger for the use of belowground carbohydrates, the lack of it in the model complicates the modeling of carbohydrate transport.

Inclusion of an improved mechanism for carbohydrate transport would make the annual dynamics of eelgrass at a specific site more realistic; it is unclear, however, whether this mechanism would change the current relative ranking of site suitability.

Conclusions and Recommendations

We adapted an eelgrass biomass model for use in Puget Sound, with the most notable improvements in how productivity is modeled using locally-collected data. However, uncertainty remains high about many components of the model given the limited data available. Improvements to some mechanisms and the addition of some potentially useful features were not possible in the scope of this project. Model accuracy as measured against monitoring data is relatively low, but predictive capability improved over the initial model. Given limitations in the model validation data and process, the

quantitative model validation should not be used as a yes/no test of model utility. Qualitatively, it is apparent that the model is more successful in some areas than others, and examination of what areas are predicted better or worse than others will help to understand the capabilities and limitations of the model and its potential use.

We believe that the current version of the eelgrass biomass model can be useful for identifying restoration sites in conjunction with other tools. The model should be applied in conjunction with field knowledge and common sense. It is worth remembering that given the availability and quality of input data, the biomass model best reflects the suitability of a site in terms of temperature, salinity, and light as integrated over the course of a year. This gives it advantage over static suitability models that consider summary metrics of water temperature and/or salinity and are less able to capture the dynamic nature of environmental quality at a site. There are other factors relevant to site suitability for eelgrass, but given an understanding that the model is addressing specific environmental factors, it can be used together with tools such as filters for substrate suitability or localized stressors.

We faced limitations in the availability of light attenuation data, such that the temporal and spatial variability of water quality is underestimated in this model. Given the importance of light to eelgrass productivity, this limitation is important, but we took steps as we were able to improve the quality of light attenuation data, and data collected locally or regionally in the future could be readily incorporated.

The model is also a useful tool for identifying areas where additional data could be used to improve model predictions. Data availability for eelgrass dynamics in Puget Sound is limited, and even some relatively simple experiments or observations could improve the model fitting and parameterization process. Similarly, data on eelgrass biomass under different conditions could improve our ability to validate the model against the same metric used as the model state variable.

Acknowledgements

References

Aveytua-Alcazar L, VF Camacho-Ibar, AJ Souza, JI Allen, and R Torres. 2008. "Modelling Zostera Marina and Ulva Spp. In a Coastal Lagoon." *Ecological Modelling* 218:354-366.

Bocci M, G Coffaro, and G Bendoricchio. 1997. "Modelling Biomass and Nutrient Dynamics in Eelgrass (Zostera Marina L.): Applications to the Lagoon of Venice (Italy) and Oresund (Denmark)." *Ecological Modelling* 102:67-80.

Burd AB and KH Dunton. 2001. "Field Verification of a Light-Driven Model of Biomass Changes in the Seagrass Halodule Wrightii." *Marine Ecology Progress Series* 209:85-98.

Carr JA, P D'Odorico, KJ McGlathery, and PL Wiberg. 2012. "Stability and Resilience of Seagrass Meadows to Seasonal and Interannual Dynamics and Environmental Stress." *Journal of Geophysical Research-Biogeosciences* 117.

Cerco C and T Cole. 1994. Three-Dimensional Eutrophication Model of Chesapeake Bay. Vicksburg, Mississippi.

Chen CS, HD Liu, and RC Beardsley. 2003. "An Unstructured Grid, Finite-Volume, Three-Dimensional, Primitive Equations Ocean Model: Application to Coastal Ocean and Estuaries." *Journal of Atmospheric and Oceanic Technology* 20:159-186.

Davies-Colley RJ, WN Vant, and DG Smith. 1993. Colour and Clarity of Natural Waters. Ellis Horwood, New York.

Eldridge PM, JE Kaldy, and AB Burd. 2004. "Stress Response Model for the Tropical Seagrass Thalassia Testudinum: The Interactions of Light, Temperature, Sedimentation, and Geochemistry." *Estuaries* 27:923-937.

Flater D. 1996. "A Brief Introduction to Xtide." *Linux Journal*:51-57.

Hemminga MA and CM Duarte. 2000. Seagrass Ecology. Cambridge University Press.

Kaldy JE and PM Eldridge. 2006. Development of Mechanistic Models to Guide Establishment of Protective Criteria for Seagrasses. US Environmental Protection Agency, Newport, OR.

Khangaonkar T, B Sackmann, W Long, T Mohamedali, and M Roberts. 2012. "Simulation of Annual Biogeochemical Cycles of Nutrient Balance, Phytoplankton Bloom(S), and Do in Puget Sound Using an Unstructured Grid Model." *Ocean Dynamics* 62:1353-1379.

Khangaonkar T, ZQ Yang, T Kim, and M Roberts. 2011. "Tidally Averaged Circulation in Puget Sound Sub-Basins: Comparison of Historical Data, Analytical Model, and Numerical Model." *Estuarine Coastal and Shelf Science* 93:305-319.

Kirk JTO. 1994. Light and Photosynthesis in Aquatic Ecosystems. 2nd edition. Cambridge University Press, New York.

Loos EA and M Costa. 2010. "Inherent Optical Properties and Optical Mass Classification of the Waters of the Strait of Georgia, British Columbia, Canada." *Progress in Oceanography* 87:144-156.

Mohamedali T, M Roberts, S B.S., and K A. 2011. Puget Sound Dissolved Oxygen Model: Nutrient Load Summary for 1999-2008. Publication No. 11-03-057, Washington State Department of Ecology, Olympia, WA.

Orth RJ. 1977. "Effect of Nutrient Enrichment on Growth of Eelgrass-Zostera-Marina in Chesapeake Bay, Virginia, USA." *Marine Biology* 44:187-194.

Pedersen MF and J Borum. 1992. "Nitrogen Dynamics of Eelgrass Zostera-Marina During a Late Summer Period of High Growth and Low Nutrient Availability." *Marine Ecology Progress Series* 80:65-73.

Romero J, KS Lee, M Perez, MA Mateo, and T Alcoverro. 2006. Nutrient Dynamics in Seagrass Ecosystems. Pages 227-254 *in* AWD Larkum, RJ Orth, and CM Duarte, editors. Seagrasses: Biology, Ecology and Conservation. Springer.

Short FT. 1987. "Effects of Sediment Nutrients on Seagrasses - Literature-Review and Mesocosm Experiment." *Aquatic Botany* 27:41-57.

Short FT, RC Davis, BS Kopp, CA Short, and DM Burdick. 2002. "Site-Selection Model for Optimal Transplantation of Eelgrass Zostera Marina in the Northeastern Us." *Marine Ecology Progress Series* 227:253-267.

Thom RM and RG Albright. 1990. "Dynamics of Benthic Vegetation Standing-Stock, Irradiance, and Water Properties in Central Puget Sound." *Marine Biology* 104:129-141.

Thom RM, AB Borde, S Rumrill, DL Woodruff, GD Williams, JA Southard, and SL Sargeant. 2003. "Factors Influencing Spatial and Annual Variability in Eelgrass (Zostera Marina L.) Meadows in Willapa Bay, Washington, and Coos Bay, Oregon, Estuaries." *Estuaries* 26:1117-1129.

Thom RM, AB Borde, GD Williams, JA Southard, SL Blanton, and DL Woodruff. 2001. Effects of Multiple Stressors on Eelgrass Restoration Projects.*in* Proceedings of the Puget Sound Research Conference. Puget Sound Action Team., Olympia, WA.

Thom RM, KE Buenau, C Judd, and VI Cullinan. 2011. Eelgrass (Zostera Marina L.) Stressors in Puget Sound., DNR Nearshore Habitat Program., Olympia, WA.

Thom RM, SL Southard, AB Borde, and P Stoltz. 2008. "Light Requirements for Growth and Survival of Eelgrass (Zostera Marina L.) in Pacific Northwest (USA) Estuaries." *Estuaries and Coasts* 31:969-980.

Williams SL and MH Ruckelshaus. 1993. "Effects of Nitrogen Availability and Herbivory on Eelgrass (Zostera-Marina) and Epiphytes." *Ecology* 74:904-918.

Yang Z and T Khangaonkar. 2010. "Multi-Scale Modeling of Puget Sound Using an Unstructured-Grid Coastal Ocean Model: From Tide Flats to Estuaries and Coastal Waters." *Ocean Dynamics* 60:1621-1637.

Zharova N, A Sfriso, A Voinov, and B Pavoni. 2001. "A Simulation Model for the Annual Fluctuation of Zostera Marina Biomass in the Venice Lagoon." *Aquatic Botany* 70:135-150.

Zimmerman RC, RD Smith, and RS Alberte. 1987. "Is Growth of Eelgrass Nitrogen-Limited: A Numerical Simulation of the Effects of Light and Nitrogen on the Growth Dynamics of *Zostera Marina*." *Marine Ecology Progress Series* 41:167-176.

Table 1(a) Model calibration error statistics for water surface elevation.

Station	MAE (m)	RMSE (m)	RME (%)
Port Angeles	0.21	0.26	6.46
Friday Harbor	0.29	0.36	9.87
Cherry Point	0.35	0.43	10.26
Port Townsend	0.24	0.29	7.64
Seattle	0.31	0.37	8.66
Tacoma	0.31	0.37	8.80
Mean	**0.29**	**0.35**	**8.48**
MAE = mean absolute error; RMSE = root mean square error			
RME = mean error relative to tidal range at each site			

Table 1(b) Model calibration error statistics for salinity and temperature.

Station	Salinity, psu		Temperature, ˚C	
	ME (psu)	RMSE (psu)	ME (˚C)	RMSE (˚C)
Admiralty Inlet Entrance (ADM2)	-0.77	0.87	0.26	0.45
Admiralty Inlet North (ADM1)	-0.57	0.82	0.21	0.48
Admiralty Inlet South (ADM3)	-0.65	0.89	0.19	0.30
Puget Sound Main Basin (PSB003)	-0.82	1.28	0.21	0.44
East Passage (EAP001)	-0.69	0.88	0.32	0.54
Hood Canal (HCB003)	-0.6	0.77	-.37	0.89
Saratoga Passage (SAR003)	-0.55	0.83	0.38	0.79
Gordon Point (GOR1), South Sound	-0.57	0.72	0.00	0.41
Nisqually Reach (NSQ002)	-0.72	0.83	0.00	0.39
Dana Passage (DNA)	-0.84	0.93	-0.17	0.63
Mean	**-0.68**	**0.88**	**0.10**	**0.532**
MAE = mean absolute error; RMSE = root mean square error				

Table 2. Attenuation coefficients used for regions of Puget Sound, calculated from Secchi depths taken at marine water quality monitoring stations.

Location	ID	Jan	Feb	Mar	Apr	May	Jun	Jul	Aug	Sep	Oct	Nov	Dec
Bellingham Bay	BLL011	0.383	0.571	0.414	0.666	0.406	0.723	0.414	0.434	0.470	0.633	0.233	0.375
Budd Inlet	BUD005	0.288	0.276	0.248	0.351	0.371	0.349	0.349	0.483	0.453	0.312	0.264	0.286
East Sound	EAS001	0.072	0.124	0.199	0.277	0.388	0.288	0.157	0.299	0.161	0.315	0.098	0.112
Elliot Bay	ELB015	0.269	0.210	0.170	0.194	0.219	0.222	0.028	0.140	0.119	0.070	0.160	0.190
Gordon Point	GOR001	0.302	0.203	0.162	0.181	0.140	0.133	0.118	0.125	0.148	0.188	0.189	0.317
Hood Canal Great Bend	HCB004	0.378	0.370	0.344	0.295	0.268	0.287	0.322	0.347	0.377	0.348	0.301	0.287
Hood Canal, Eldon	HCB003	0.224	0.288	0.334	0.240	0.206	0.239	0.211	0.238	0.337	0.299	0.134	0.389
Liberty Bay	POD006	0.398	0.340	0.344	0.364	0.375	0.375	0.357	0.441	0.445	0.394	0.441	0.544
Nisqually Reach - Devils Head	NSQ002	0.257	0.185	0.159	0.230	0.204	0.213	0.177	0.180	0.182	0.169	0.168	0.202
Nisqually River Delta	NSQ001	0.445	0.311	0.336	0.420	0.450	0.354	0.117	0.143	0.179	0.410	1.167	1.080
Penn Cove Park	PNN001	0.321	0.161	0.344	0.220	0.457	0.309	0.420	0.434	0.352	0.288	0.273	0.255
Port Madison	PMA001	0.173	0.160	0.220	0.167	0.173	0.294	0.233	0.267	0.160	0.194	0.215	0.229
Possession Sound	PSS019	0.379	0.282	0.409	0.388	0.342	0.378	0.337	0.315	0.326	0.232	0.356	0.336
Skagit Bay Hope Island	SKG001	0.513	0.537	0.465	0.292	0.398	0.525	0.406	0.513	0.550	0.436	0.432	0.502
Skagit Bay Str Point	SKG003	0.453	0.517	0.489	0.445	0.390	0.511	0.581	0.447	0.511	0.378	0.347	0.523

Table 3. Photosynthesis-irradiance model fits and Akaike Information Criteria statistics corrected to small sample sizes (AIC$_c$). Surfaces were fit to data collected by Thom et al. (2008; unpublished). Two P-I curves (Smith-Talling and Jassby-Platt) were tested. P$_{max}$ depended on temperature with either an exponential or quadratic relationship. The shape parameters for the P-I curves (α and I$_k$) were either held constant or linearly dependent upon temperature. Bold type indicates the model used to calculate gross primary production in the biomass model.

P$_{max}$-temperature relationship	Photsynthesis-irradiance formulation	SSE	R^2	k	AICc	delta AIC	weight
exponential	Jassby-Platt, linear I$_k$	0.000938	0.1532	4	-359.12	7.83	0.01
exponential	Smith-Talling, linear α	0.000962	0.1315	4	-358.23	8.71	0.01
quadratic	Jassby-Platt, linear I$_k$	0.000759	0.3151	5	-363.81	3.14	0.09
quadratic	**Jassby-Platt, constant I$_k$**	**0.000762**	**0.3124**	**4**	**-366.41**	**0.54**	**0.34**
quadratic	Smith-Talling, linear α	0.000748	0.325	5	-364.33	2.62	0.12
quadratic	Smith-Talling, constant α	0.00075	0.3229	4	-366.95	0.00	0.44

Table 4. State variables, forcing variables, and parameters for eelgrass biomass model.

Description	Symbol	Value	Unit
Aboveground biomass	C_a	variable	mol C m^{-2}
Belowground biomass	C_b	variable	mol C m^{-2}
Photosynthetically active radiation	I	time series	mol photons m^{-2} day^{-1}
Temperature	T	time series	degrees C
Salinity	S	time series	ppt
Attenuation coefficient	K_{PAR}	see Table 2	m^{-1}
Time step	Δt	1	hr
Translocation coefficient	τ	0.5	unitless
Exudation coefficient	δ	0.000275	unitless
Density dependence coefficient	κ	6	mol C m^{-2}
Maximum photosynthesis rate	P_{max}		molC mol C^{-1} hr^{-1}
Quadratic term	β_{p2}	-4.677×10^{-5}	
Linear term	β_{p1}	0.00149	
Intercept	β_{p0}	-0.003126	
Light saturation parameter	I_k	7.024	mol m^{-2} hr^{-1}
Salinity multiplier			unitless
Slope	β_{s1}	0.029	
Intercept	β_{s0}	0.13	
Respiration	R		molC mol C^{-1} hr^{-1}
Slope/Exponential term	β_{r1}	-0.000236	
Intercept/Coefficient	β_{r0}	0.00148	
Belowground multiplier		1.6	unitless
Aboveground mortality	M_a	6.72×10^{-5}	hr^{-1}
Belowground mortality	M_b	7.92×10^{-5}	hr^{-1}

Figure 1. PSGB model grid along with water quality monitoring stations used in model calibration.
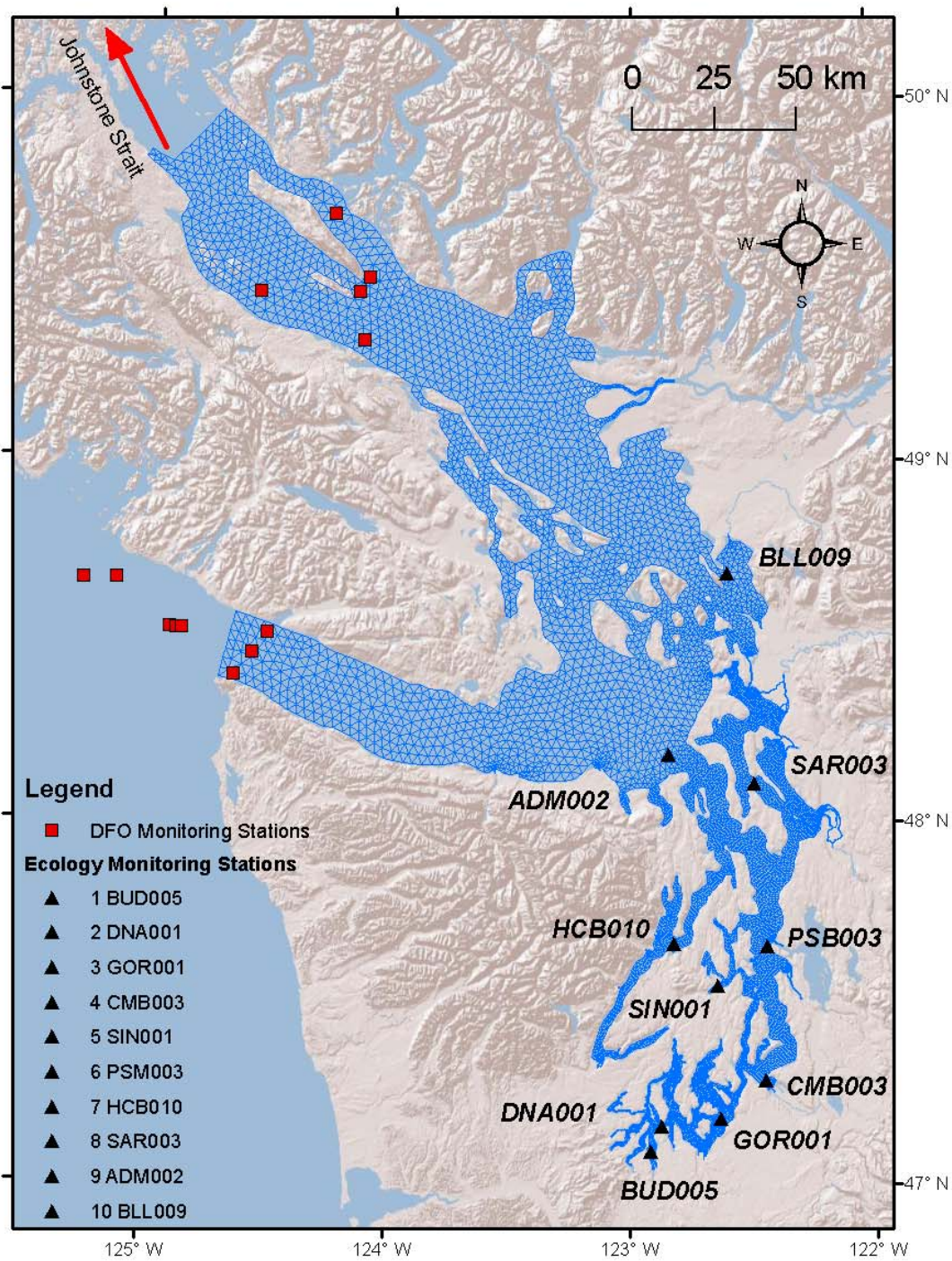
Figure 2. Comparison of simulated tides (in NAVD88), salinity, and temperature with NOAA XTide and monthly monitoring data collected by Washington State Department of Ecology.

(a)
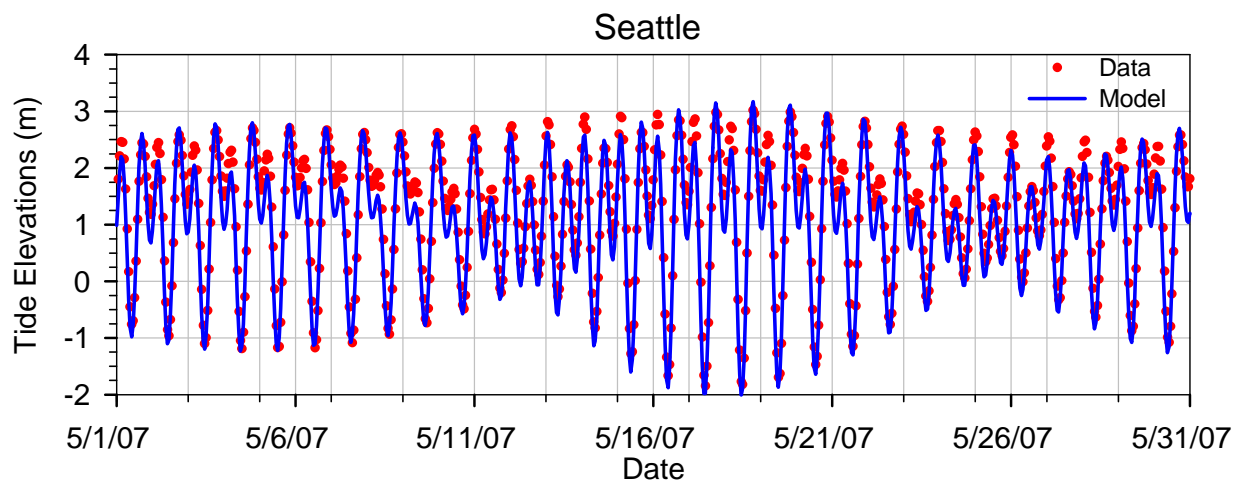
(b)
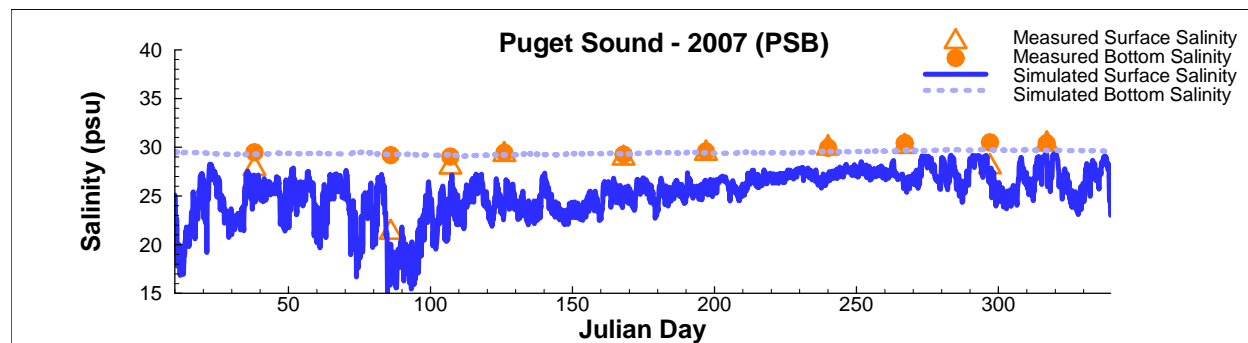
(c)
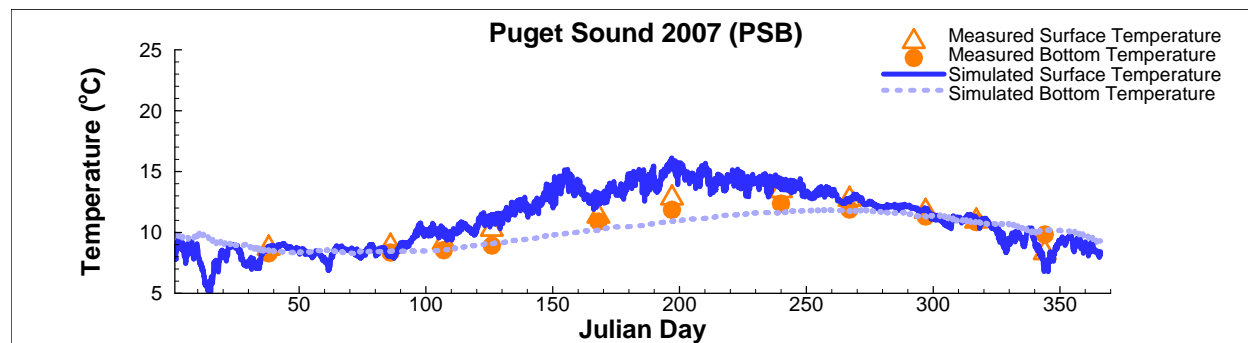
Figure 3. Map of regions for attenuation coefficients. Labels are station IDs as listed in Table 2. All areas not contained in a polygon use the attenuation data for station EAS001.
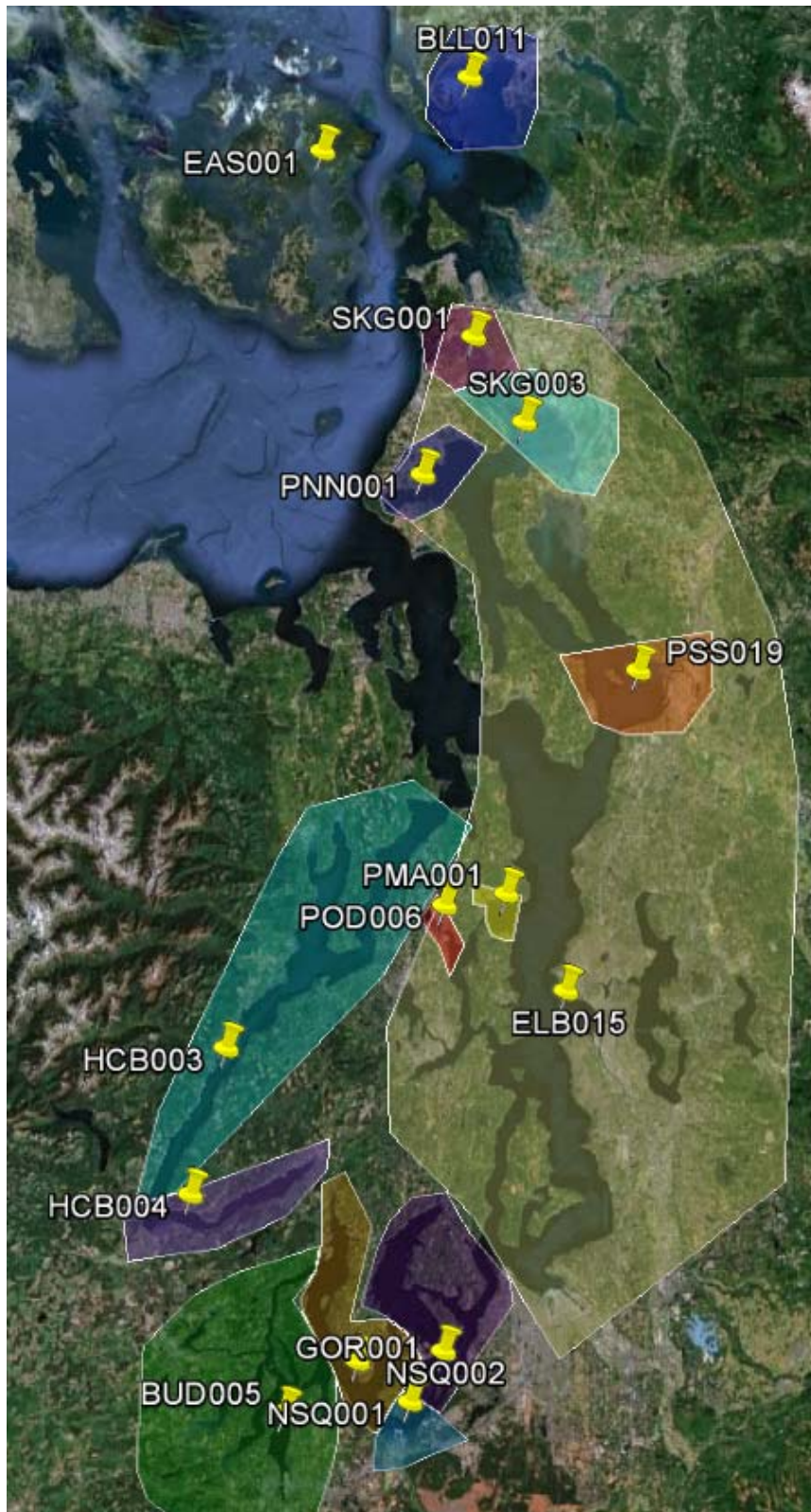
Figure 4. Data used to determine relationship of gross primary production to temperature and light. Surface is equation 7 fit to the experimental data.
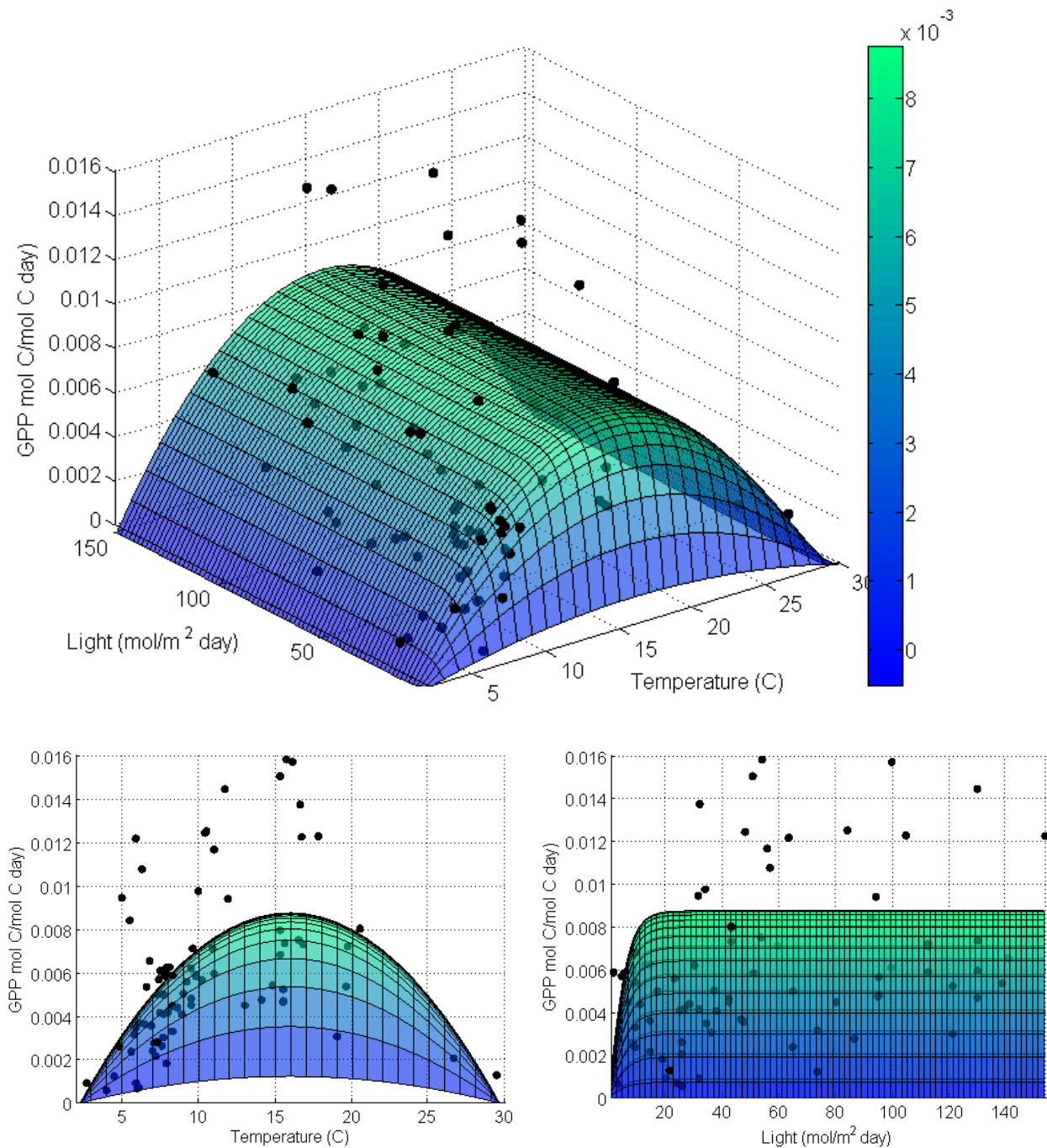
Figure 5. Experimental results from eelgrass held in various salinity treatments for 24 or 67 hours. Data shown are percent reductions in gross primary productivity (GPP) from maximum production at 30 ppt. Consequently, the fitted line (R^2 = 0.82) is constrained to 1 when salinity is 30 ppt.
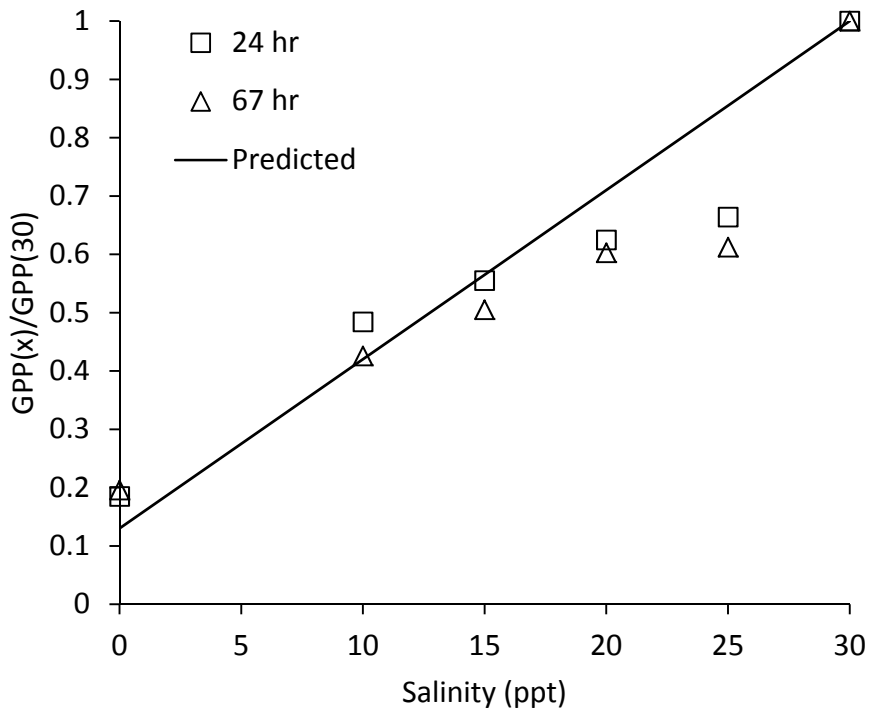
Figure 6. Experimental data used to determine temperature-respiration relationship, with best-fit linear regression (R^2 = 0.85).
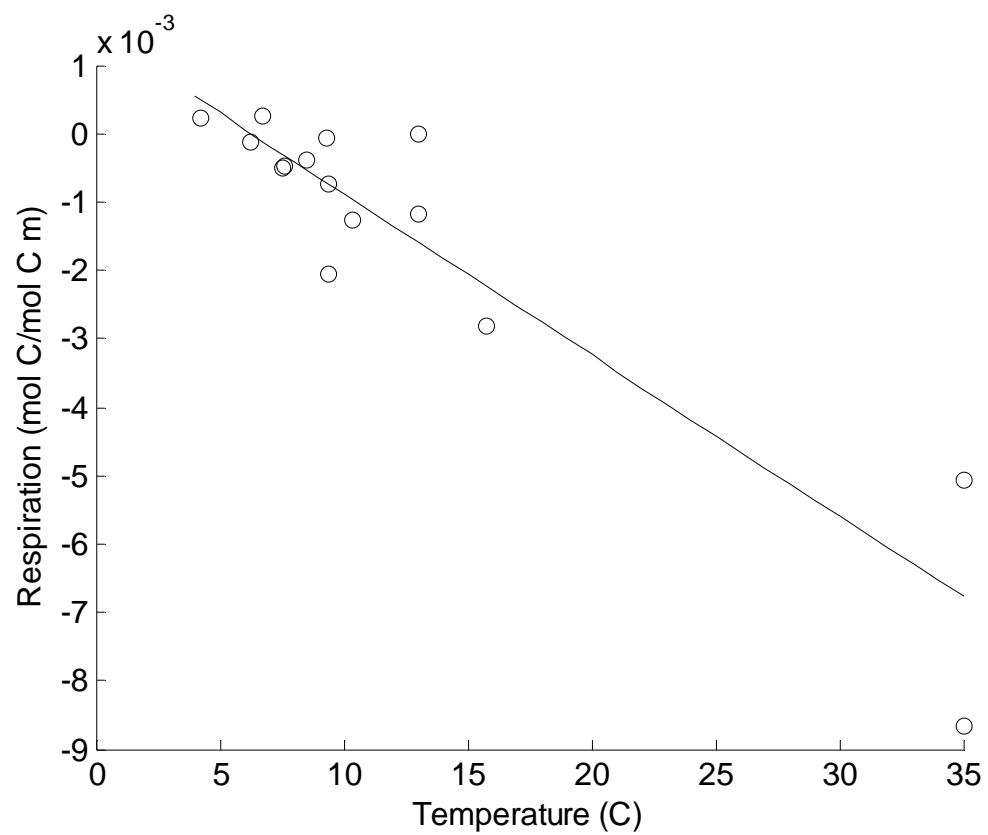
Figure 7. Model results from single site (Sequim Bay) at depth of -3m NAVD88. Light, water temperature, attenuation coefficients and salinity inputs to the eelgrass biomass model; gross photosynthesis, respiration, growth rate, and biomass are outputs from the model.
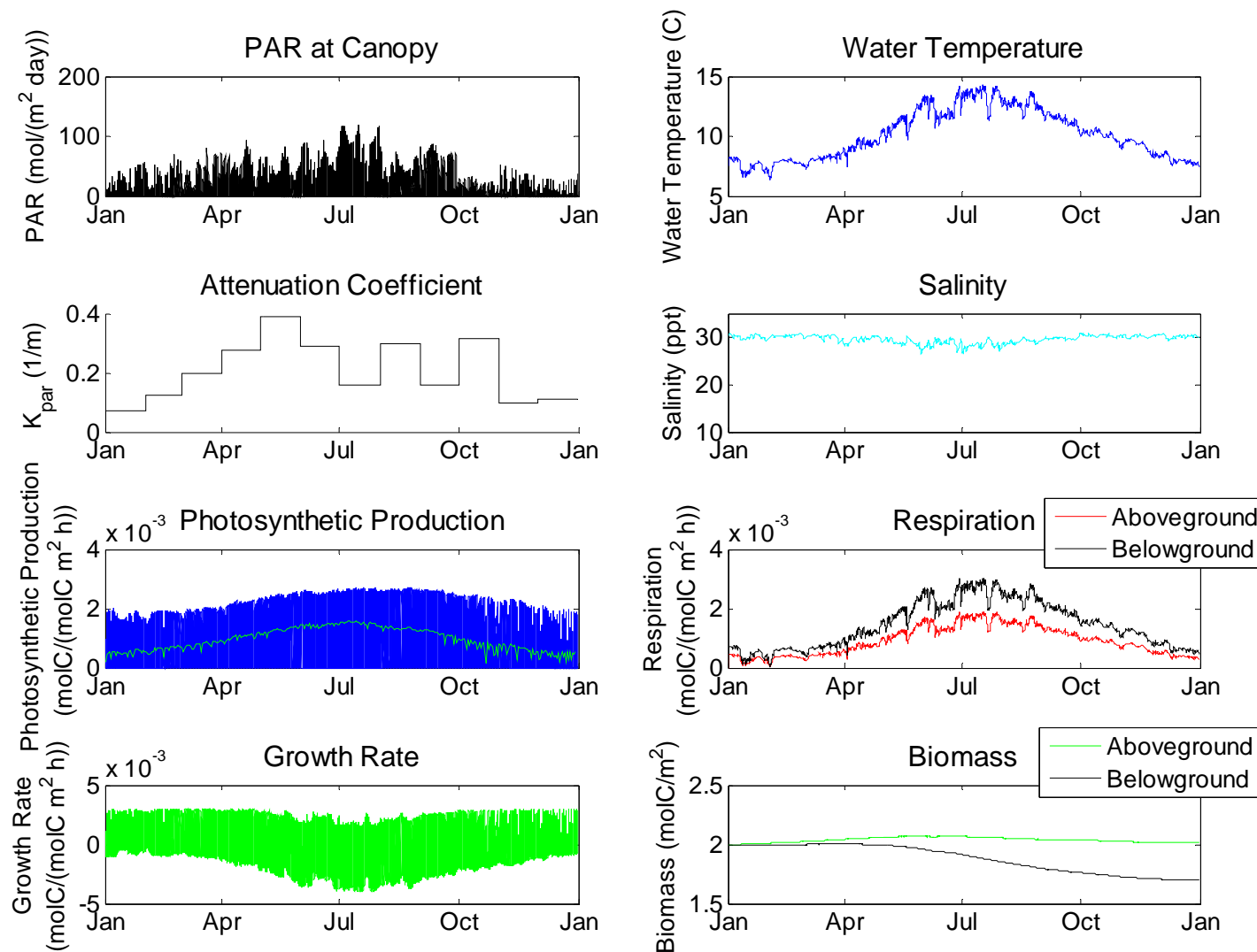
Figure 8. Comparison of model results from Sequim Bay (thick lines) and Hood Canal (Great Bend; thin lines) at depth of -3m NAVD88. Light, water temperature, attenuation, and salinity are inputs to the eelgrass biomass model; gross photosynthesis, respiration, growth rate, and biomass are outputs from the model.
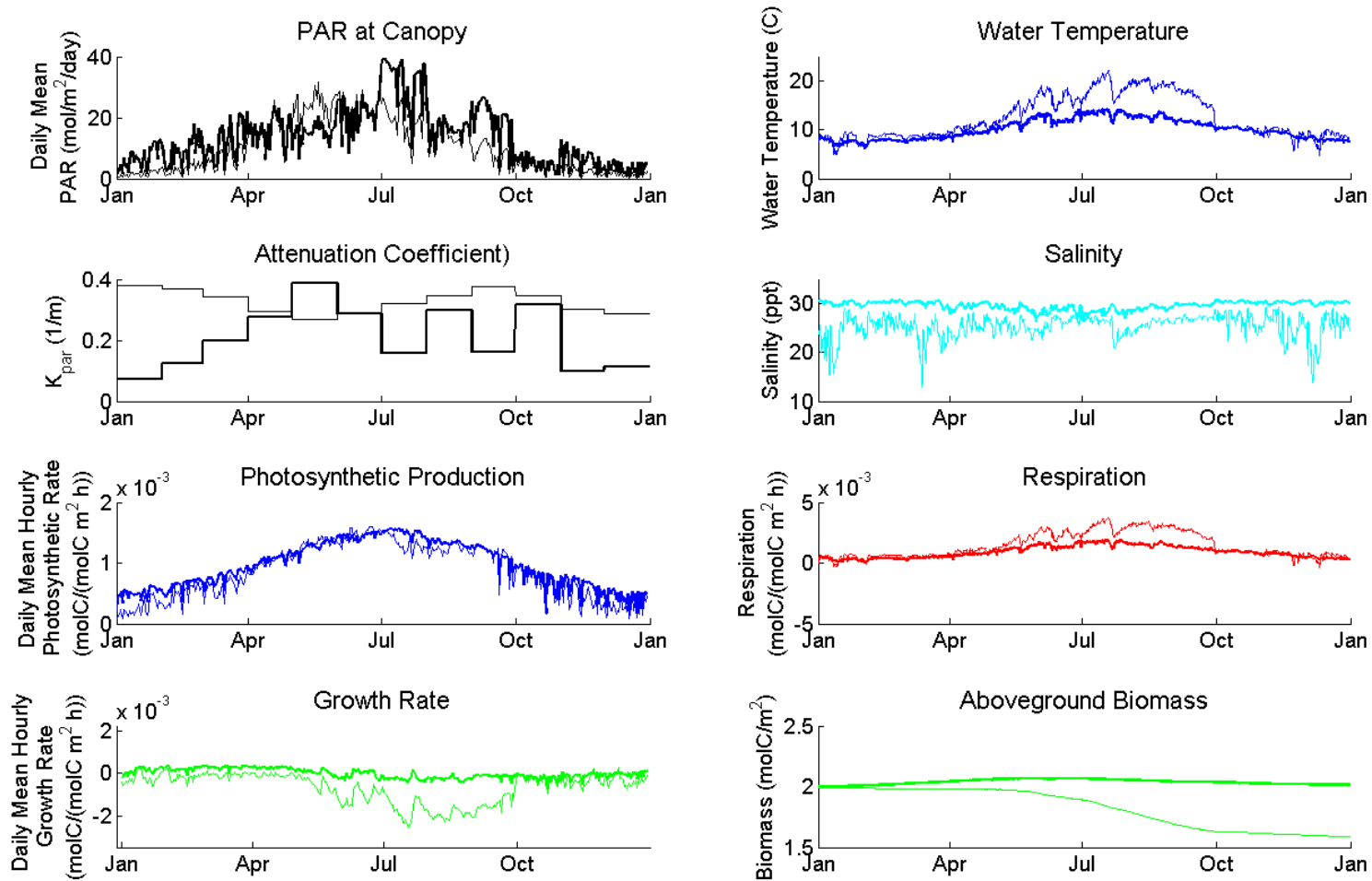
Figure 9. Mean and maximum water temperature (°C) inputs to eelgrass model. Note difference in color scale.
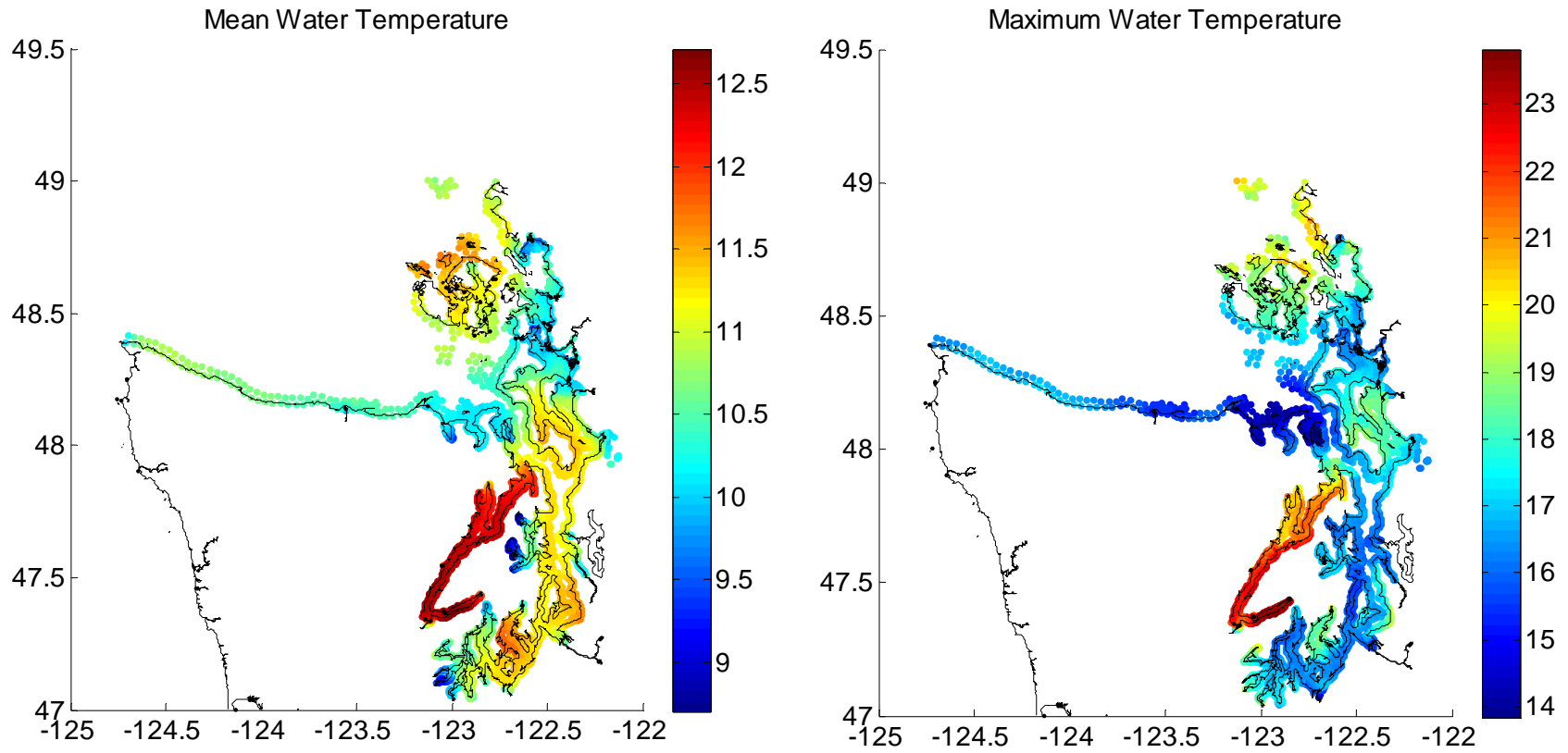
Figure 10. Mean and minimum salinity (ppt) inputs to eelgrass model.
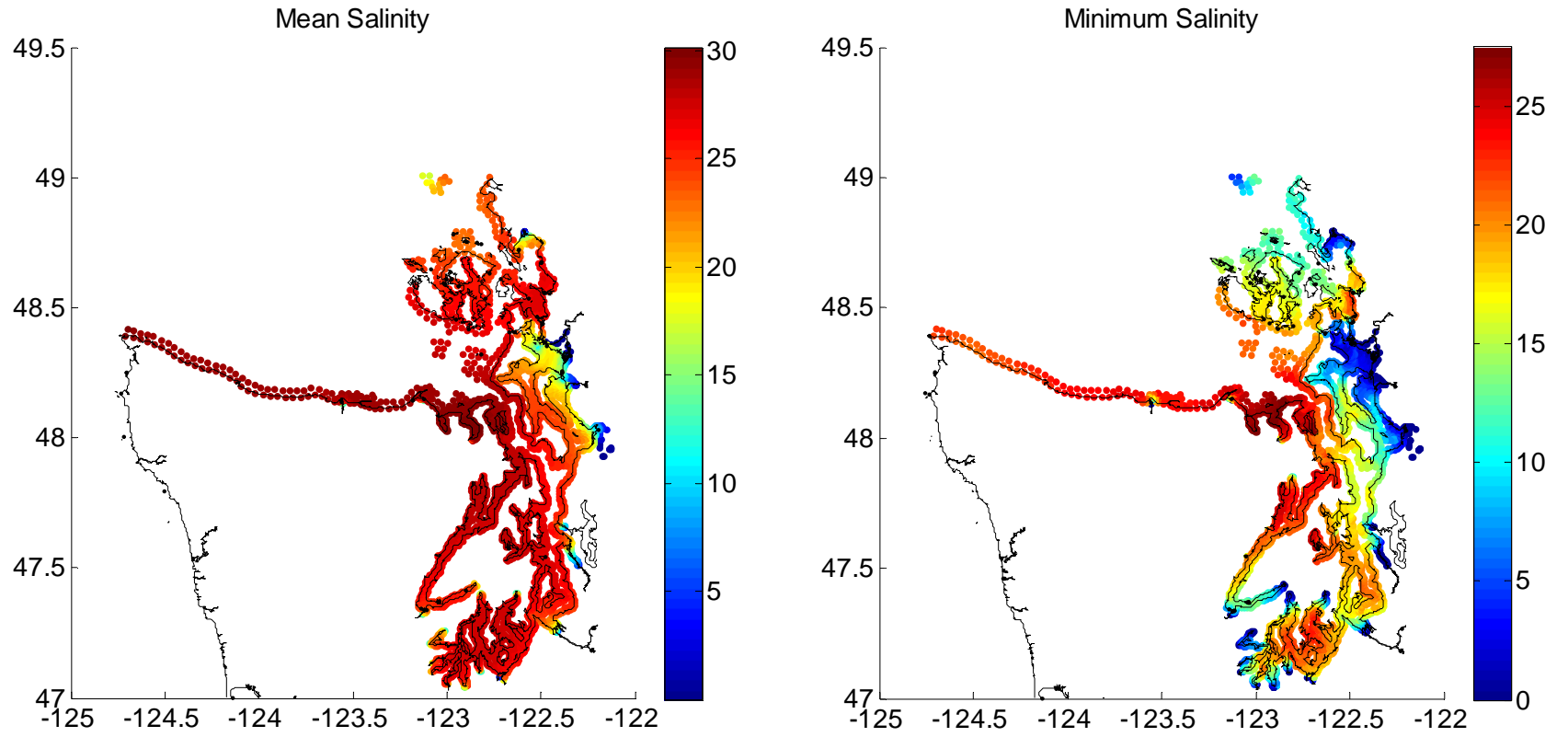
Figure 11. Mean and maximum attenuation coefficients (K_{PAR}; m^{-1}) used in eelgrass model. Note differences in color scale.
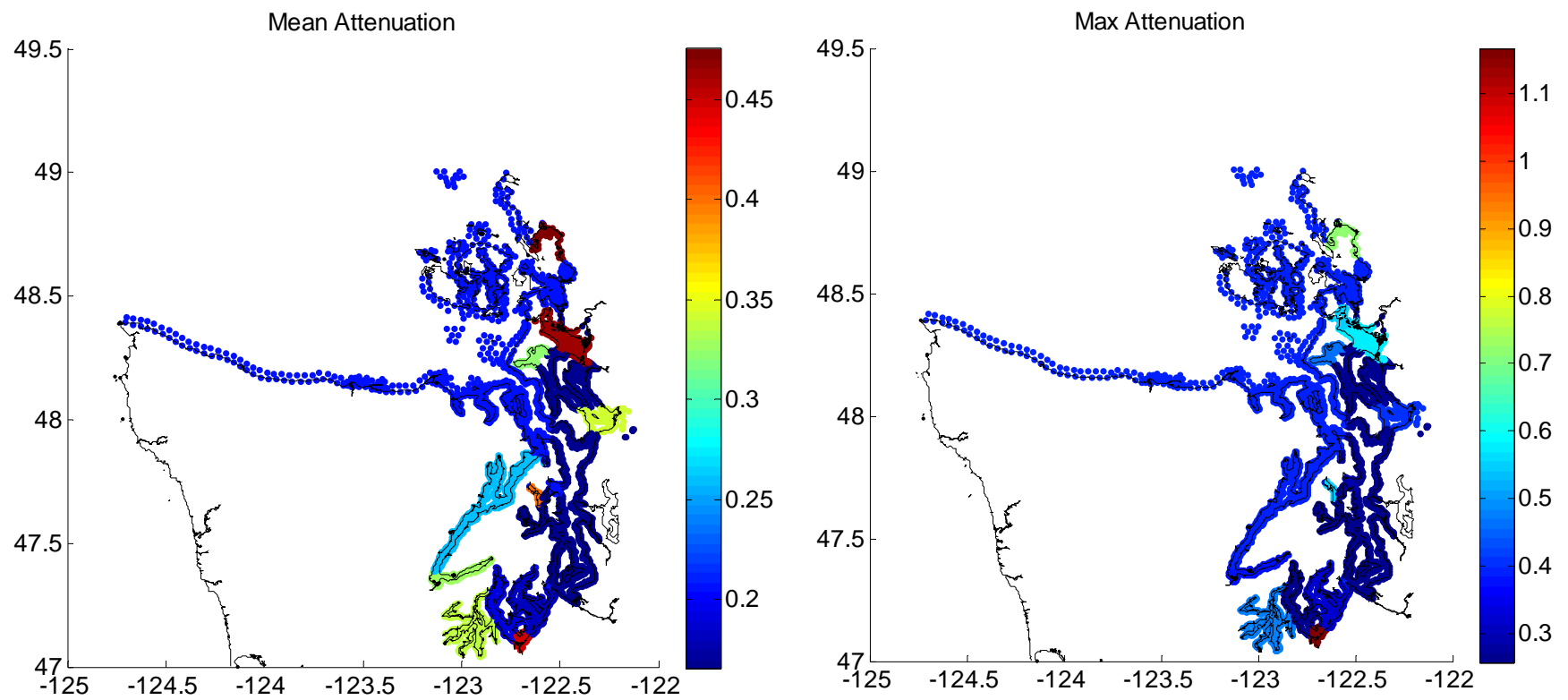
Figure 12. Eelgrass biomass (molC/m^2) after one calendar year (2007) at a canopy depth of -1m NAVD88. Initial biomass is 2 molC/m^2.
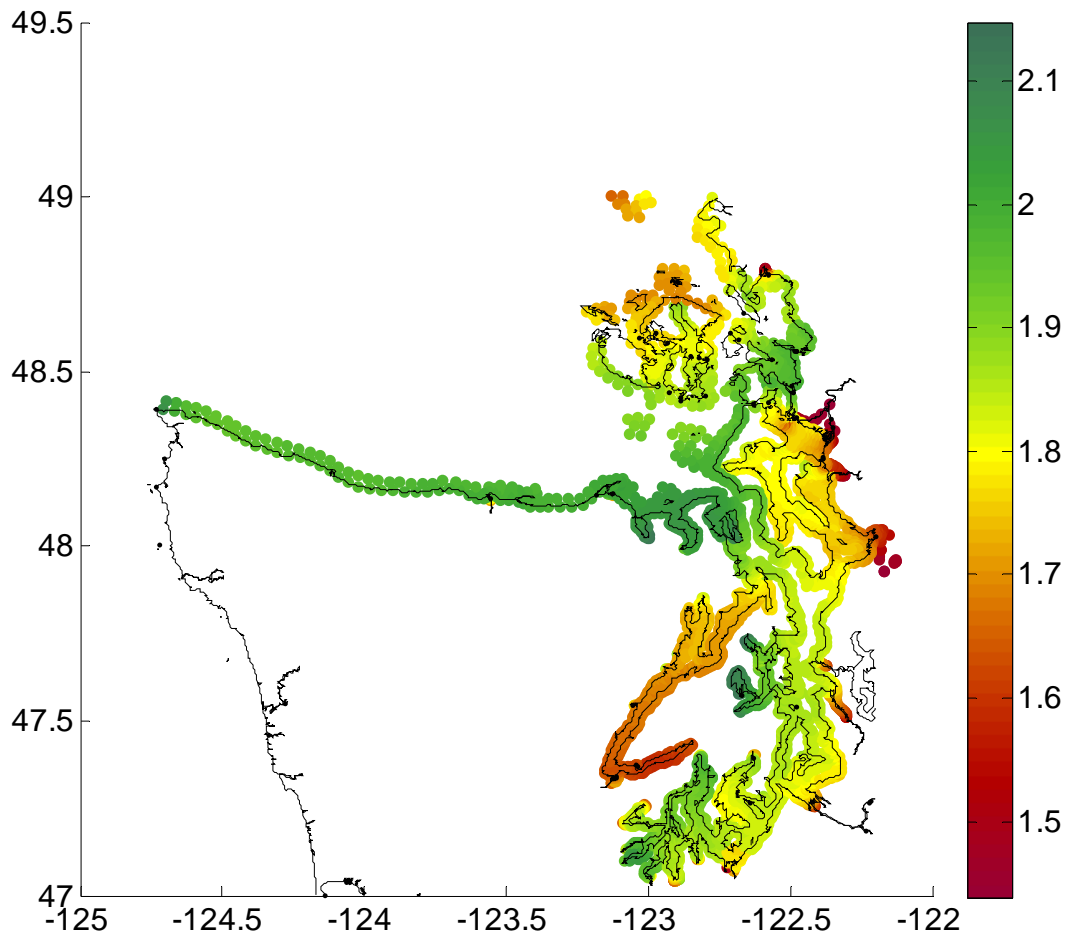
Figure 13. Eelgrass biomass (molC/m^2) after one calendar year (2007) at a canopy depth of -3m NAVD88. Initial biomass is 2 molC/m^2.
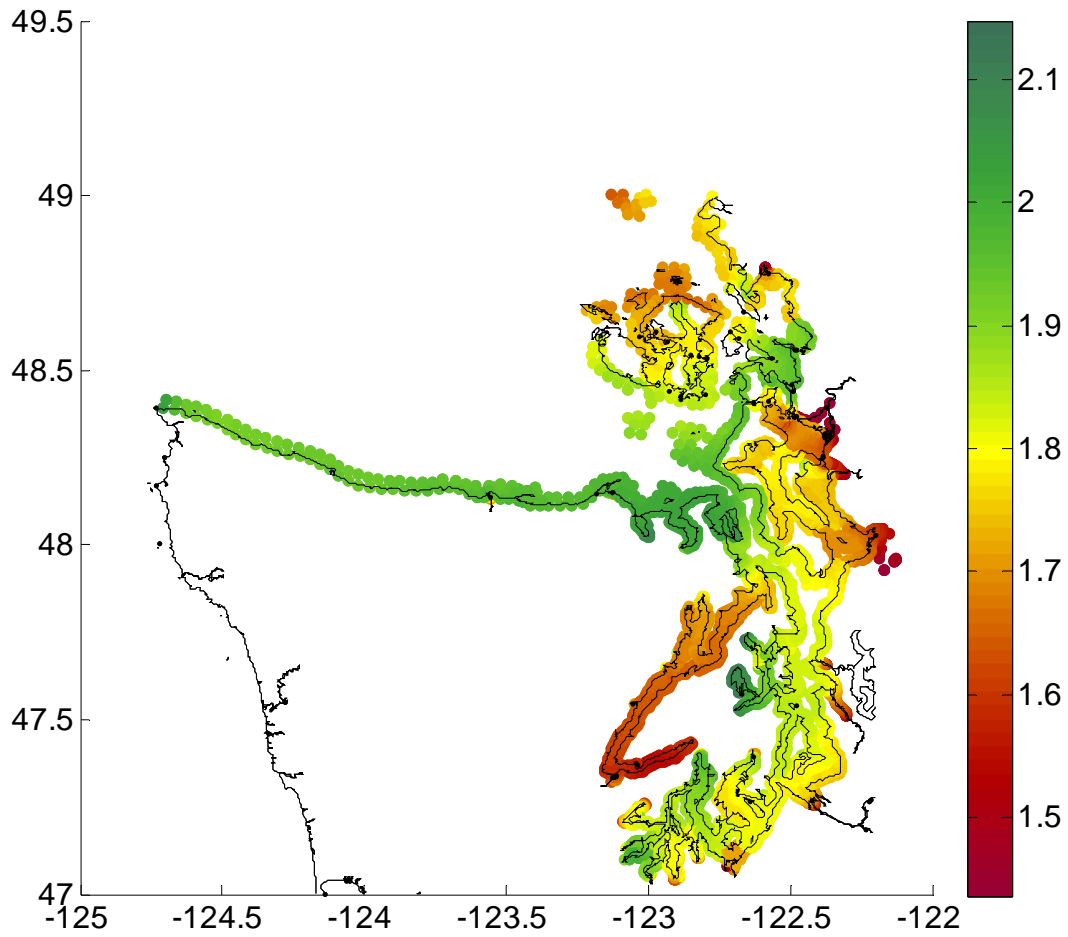
Figure 14. Eelgrass biomass (molC/m^2) after one calendar year (2007) at a canopy depth of -5m NAVD88. Initial biomass is 2 molC/m^2.
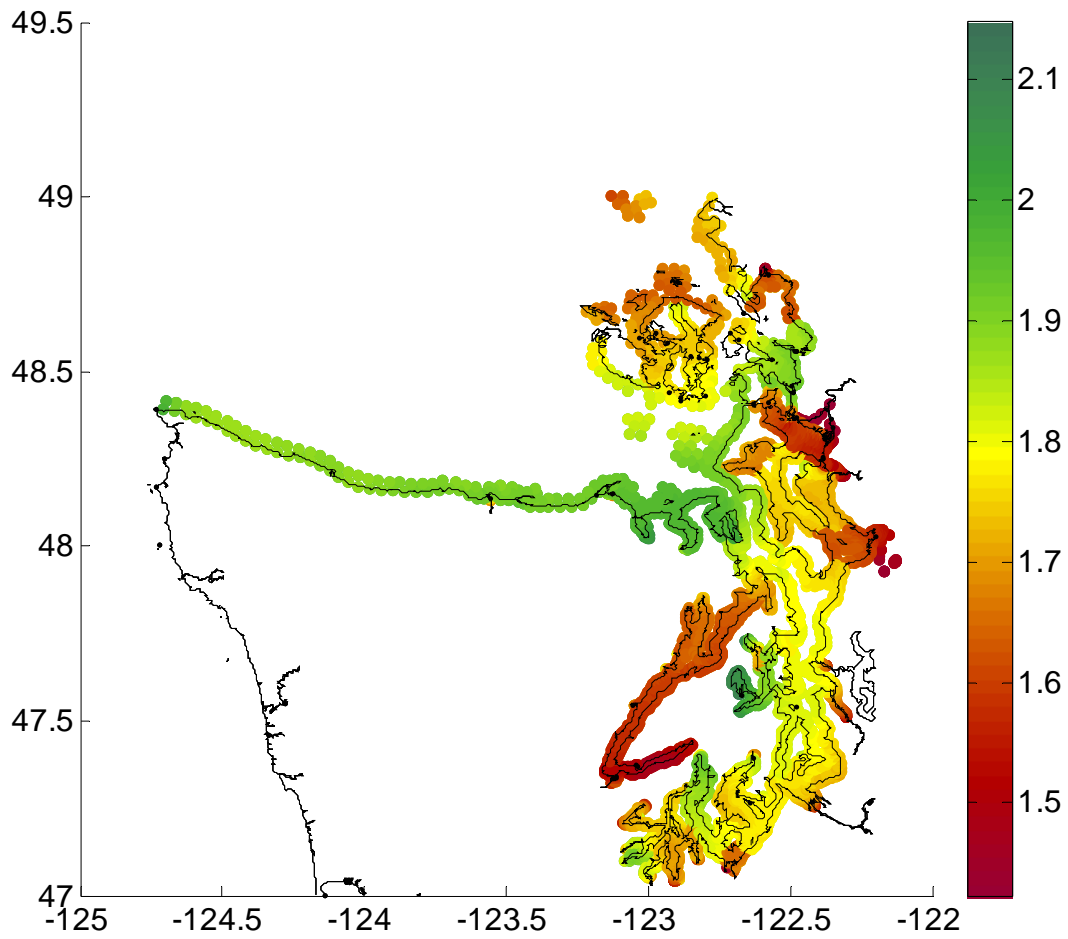
Figure 15. Final eelgrass biomass plotted against model inputs for 2007. Results are generated for -3m NAVD88.
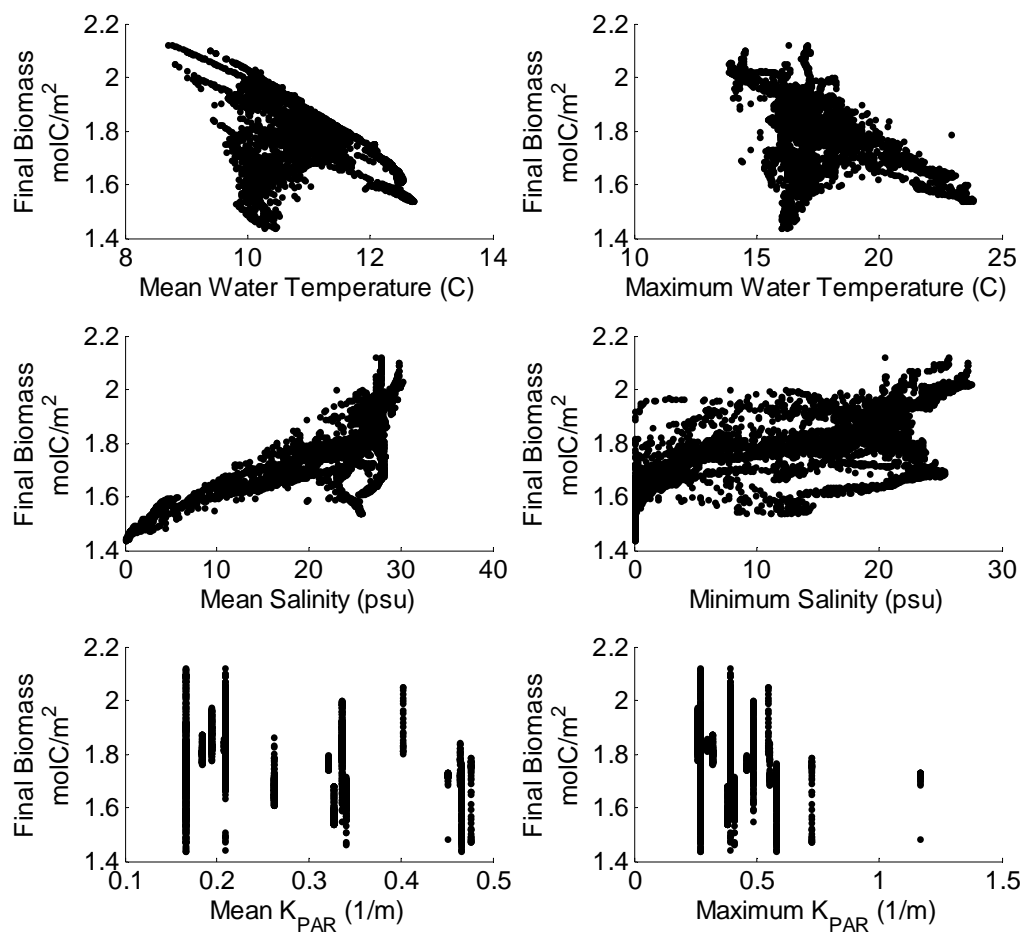
Figure 16. Model validation results for northern Puget Sound for model run at -3m NAVD88 in 2007. Similarity of color between outer and inner circle indicates agreement of model and monitoring data; contrast in color indicates disagreement. Both monitoring data (percent cover) and model results (biomass) are indexed from 0-1 for comparison purposes. Light outer circles and dark inner circles may indicate suitable sites for eelgrass transplant.
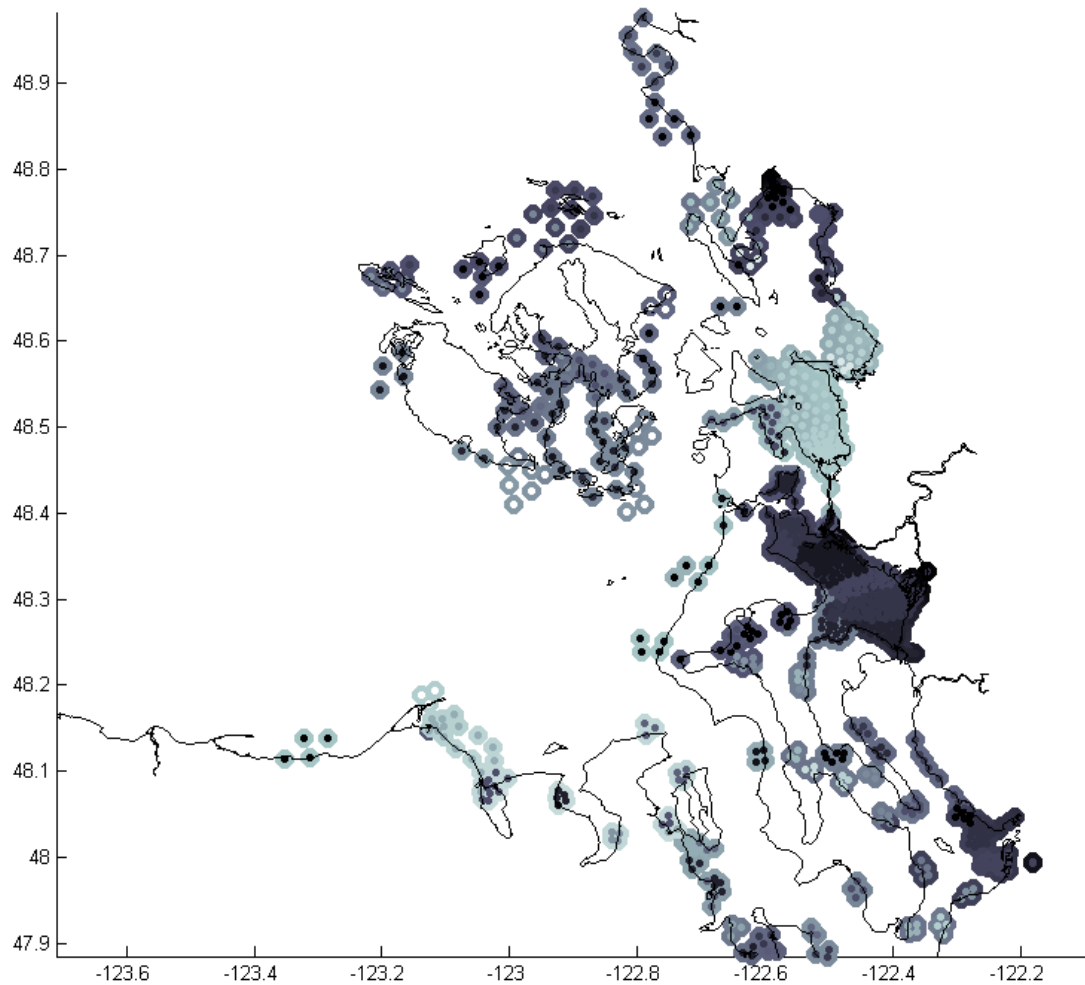
Outer circle indicates model prediction
Inner circle indicates percent cover estimate
Both are scaled 0-1
Similar colors = agreement

○ Model predicts high, percent cover is high

⊛ Model predicts high, percent cover is low

◎ Model predicts low, percent cover is high

⬤ Model predicts low, percent cover is low

Figure 17. Model validation results for southern Puget Sound for model run at -3m NAVD88. Similarity of color between outer and inner circle indicates agreement of model and monitoring data; contrast in color indicates disagreement. Both monitoring data (percent cover) and model results (biomass) are indexed from 0-1 for comparison purposes. Light outer circles and dark inner circles may indicate suitable sites for eelgrass transplant.

Outer circle indicates model prediction
Inner circle indicates percent cover estimate
Both are scaled 0-1
Similar colors = agreement

○ Model predicts high, percent cover is high

⊛ Model predicts high, percent cover is low

◎ Model predicts low, percent cover is high

⬣ Model predicts low, percent cover is low